kidney INTERNATIONAL ISN

Alkylating Histone Deacetylase Inhibitor treatment in experimental MPO-ANCA Vasculitis

Journal:	*Kidney International*
Manuscript ID	KI-10-17-1540.R1
Article Type:	Basic Research
Date Submitted by the Author:	04-May-2018
Complete List of Authors:	Dooley, Dearbhaile; University of Dublin Trinity College, Trinity Health Kidney Centre, Trinity Translational Medicine Institute, St. James' Hospital Campus van Timmeren, Mirjan; University Medical Center Groningen, Pathology and Medical Biology O'Reilly, Vincent; University of Dublin Trinity College, Trinity Health Kidney Centre, Trinity Translational Medicine Institute, St. James' Hospital Campus Brady, Gareth; University of Dublin Trinity College, Trinity Health Kidney Centre, Trinity Translational Medicine Institute, St. James' Hospital Campus Fazekas, Barbara; University of Dublin Trinity College, Trinity Health Kidney Centre, Trinity Translational Medicine Institute, St. James' Hospital Campus O'Brien, Eoin ; University of Dublin Trinity College, Trinity Health Kidney Centre, Trinity Translational Medicine Institute, St. James' Hospital Campus Hickey, Fionnuala; University of Dublin Trinity College, Trinity Health Kidney Centre, Trinity Translational Medicine Institute, St. James' Hospital Campus Leacy, Emma; University of Dublin Trinity College, Trinity Health Kidney Centre, Trinity Translational Medicine Institute, St. James' Hospital Campus Pusey, Charles; Imperial College London, Renal Section Tam, Frederick; Imperial College London, Renal Section, Division of Medicine Mehrling, Thomas; Mundipharma Medical Company Hamilton Bermuda Zweigniederlassung Basel Heeringa, Peter; University Medical Center Groningen, Pathology & Medical Biology - Pathology section Little, Mark; University of Dublin Trinity College, Trinity Health Kidney Centre, Trinity Translational Medicine Institute, St. James' Hospital Campus
Keywords:	ANCA, glomerulonephritis, albuminuria, inflammation, renal pathology
Subject Area:	Glomerular Disease, Immunology

SCHOLARONE™
Manuscripts

For Peer Review Only

ORIGINAL ARTICLE

Title: Alkylating Histone Deacetylase Inhibitor treatment in experimental MPO-ANCA Vasculitis

Running Title: Alkylating HDACi treatment in MPO-ANCA Vasculitis

Authors: Dearbhaile Dooley; PhD[1], Mirjan M van Timmeren[2]; PhD[2], Vincent P. O'Reilly; PhD[1], Gareth Brady; PhD[1], Eóin C. O'Brien; PhD[1], Barbara Fazekas; PhD[1], Fionnuala B. Hickey; PhD[1], Emma Leacy; BSc[1], Charles D. Pusey; PhD[3], Frederick W. K. Tam; PhD[3], Thomas Mehrling; PhD[4], Peter Heeringa; PhD[2], Mark A. Little; PhD[1,5 *]

Author affiliations

[1]Trinity Health Kidney Centre, Trinity Translational Medicine Institute, Trinity College Dublin, St. James' Hospital Campus, Ireland

[2]Department of Pathology and Medical Biology, University of Groningen, University Medical Centre Groningen, Groningen, The Netherlands

[3]Renal and Vascular Inflammation Section, Department of Medicine, Imperial College London, United Kingdom

[4]Mundipharma-EDO GmbH, Basel, Switzerland

[5]Irish Centre for Vascular Biology, Trinity College Dublin, Ireland

*Corresponding author

Prof. Mark A. Little

Trinity Health Kidney Centre, Trinity Translational Medicine Institute, Trinity College Dublin, St. James' Hospital Campus, Dublin 8, Ireland

Phone: +353 1896 3706

Email: mlittle@tcd.ie

Word count = 4002

For Peer Review Only

ABSTRACT

Current therapies for treating anti-neutrophil cytoplasm autoantibody (ANCA)-associated vasculitis include cyclophosphamide and corticosteroids. Despite inducing remission in most patients, these agents are associated with severe adverse effects. Histone deacetylase inhibitors (HDACi) are effective in rodent models of inflammation and act synergistically with many pharmacological agents, including alkylating agents like cyclophosphamide. EDO-S101 is an alkylating HDACi fusion molecule combining the DNA alkylating effect of Bendamustine, with a pan-HDACi, Vorinostat. We studied the effects of EDO-S101 in two established rodent models of ANCA-associated vasculitis: a passive mouse model of anti-myeloperoxidase IgG-induced glomerulonephritis and an active rat model of anti-myeloperoxidase-ANCA microscopic polyangiitis (EAV). Although pre-treatment with EDO-S101 reduced circulating leukocytes, it did not prevent development of passive IgG-induced glomerulonephritis in mice. On the other hand, treatment in rats significantly reduced glomerulonephritis and lung haemorrhage. EDO-S101 also significantly depleted rat B and T cells, and induced DNA damage and apoptosis in proliferating human B cells, suggesting a selective effect on the adaptive immune response. Taken together, EDO-S101 may have a role in treatment of ANCA-associated vasculitis, operating primarily through its effects on the adaptive immune response to the autoantigen myeloperoxidase.

For Peer Review Only

INTRODUCTION

Anti-neutrophil cytoplasm autoantibody (ANCA)-associated vasculitis (AAV) is a systemic autoimmune condition that affects small- to medium-sized blood vessels. Severe vessel wall damage causes inflammatory necrosis and consequent loss of organ function. The lungs and kidneys are frequently affected, leading to lung haemorrhage and glomerulonephritis (GN). Patients with AAV develop circulating autoantibodies against the neutrophil granule and monocyte lysosomal enzymes myeloperoxidase (MPO) or proteinase 3 (PR3)[1,2]. Conventional treatment includes cyclophosphamide and corticosteroids, which induces remission in most patients. However, these therapies do not fully prevent disease relapse and patients often require long-term treatment, which is associated with severe morbidity[3]. This highlights the urgent need for development of new therapies.

Histone deacetylase inhibitors (HDACi) were originally described as a class of anti-cancer drugs in 2006 due to their growth arrest and apoptotic effects on tumour cells[4]. They target the histone deacetylase enzymes which remove the acetyl groups from lysine residues, leading to chromatin condensation and transcriptional silencing. HDACi thus result in histone hyperacetylation, thereby affecting gene transcription. This enhances activity of some transcription factors such as the tumour suppressor p53, but represses B and T-cell transcription factors. Therefore, in the setting of autoimmunity, HDACi can induce cell cycle arrest or apoptosis of key leukocyte populations that are proliferating in response to auto-antigen exposure. Recently, HDACi were shown to have beneficial effects in inflammatory rodent models, such as arthritis, asthma and colitis; however, their mechanism(s) of action are not well understood[5]. HDACi act synergistically with a diverse range of pharmacological and biological agents, including cyclophosphamide. Therefore, it appears likely that HDACi may be best used in the clinic as part of a combination regimen, enabling a multitarget approach.

For Peer Review Only

EDO-S101, a small molecule compound developed by Mundipharma GmbH, is an alkylating HDACi fusion molecule which combines the strong DNA damaging effect of Bendamustine, with a fully functional pan-HDACi, Vorinostat. This combination therapy has the potential to provide enhanced efficacy at a lower alkylating agent dose due to its bi-functional mode of action. HDAC inhibition allows for better access of the alkylating moiety to the DNA double strands by opening the chromatin, thereby creating the potential for enhanced synergy between the two moieties. EDO-S101 has demonstrated good tolerability and exerts significant activity against haematological malignancy and solid tumours[6-8].

We hypothesised that EDO-S101 is an effective therapy for AAV. To dissect its effects on both the innate and adaptive immune response, we tested its efficacy in two well established rodent models of MPO-AAV: a passive mouse model of anti-MPO IgG-induced GN and an active rat model of Experimental Autoimmune Vasculitis (EAV). EAV is an MPO-ANCA vasculitis model induced by immunisation of Wistar Kyoto (WKY) rats with hMPO, resulting in crescentic GN and lung haemorrhage. These features of mild pauci-immune vasculitis are indistinguishable pathologically from human vasculitis, making EAV a valuable pre-clinical model in AAV. We observed that EDO-S101 was largely ineffective in the murine model but dramatically improved renal and lung disease in the rat model. Thus, EDO-S101 shows potential as a novel treatment for AAV, largely through its action on the adaptive immune response.

For Peer Review Only

RESULTS

EDO-S101 induces global H3 hyperacetylation in HL60 Cells and a strong DNA repair response *in vivo*

Hyperacetylation of the Histone3 (H3) tail at lysine residues K9, K14, K23 and K56 was measured using specific antibodies for acetylated lysine residues in total cell extracts of HL60 cells **(Fig. 1A).** EDO-S101 demonstrated enhanced acetylation of lysine residues, whereas Bendamustine (Bend) was equivalent to the DMSO control **(Fig. 1A)**. Exposure to EDO-S101 *in vivo* caused a strong DNA repair response (activation of p53 and pH2AX) in tumours taken at day 4 and 8 from mice bearing subcutaneous human Daudi Burkitt's lymphoma **(Fig. 1B).** Both ataxia telangiectasia mutated (ATM) kinase and Rad3-related protein (ATR) are activated upon DNA damage. Following their recruitment to DNA damage sites, ATM and ATR activate the Checkpoint Kinase 2 (Chk2) and Checkpoint kinase 1 (Chk1), respectively. These kinases were investigated as their pathways are central in DNA damage repair and their over-activation may confer aggressive molecular features, including endogenous DNA damage and oncogene-induced replication stress[9]. Taken together, these allowed us to investigate the simultaneous effects of EDO-S101 on DNA damage and blocking of damage repair. Indirect HDACi activity was measured in tumour samples on days 4 and 8; p-ATR and p-ATM were dose dependently suppressed by EDO-S101 treatment. On the other hand, p-CHK2 was strongly upregulated at day 4, but returned to undetectable levels at day 8 **(Supplemental Fig. 1A)**.

EDO-S101 has little effect on anti-MPO induced vasculitis in a passive transfer model of MPO-AAV

Given the potent combination of HDACi and alkylating capacity of the compound, we tested the ability of EDO-S101 to prevent vasculitic injury induced by anti-MPO antibodies in a passive transfer

The International Society of Nephrology (http://www.isn-online.org/site/cms)

For Peer Review Only

model, with the compound given from the time of antibody transfer. Circulating anti-MPO antibody levels were similar in vehicle and EDO-S101 pre-treated mice at day 1 and day 7 **(Fig. 2A and Supplemental Fig. 2A).** Following disease induction, both vehicle and EDO-S101 pre-treated mice developed characteristic haematuria, which decreased over time (day 1 to day 7). Although there was no significant effect on haematuria **(Supplemental Fig. 2B),** EDO-S101 reduced albuminuria compared with vehicle treated controls **(Fig. 2B)**. Both vehicle and EDO-S101 pre-treated mice developed GN **(Fig. 2D-K)**, with no significant effect of EDO-S101 on crescentic GN **(Fig. 2C)** or glomerular histopathology evident **(Supplemental Fig. 3A+B)**.

Treatment of the active model of EAV with EDO-S101 abolishes crescentic glomerulonephritis and reduces lung haemorrhage

As there was little impact of EDO-S101 on a direct antibody-induced model of vasculitis, we hypothesised that the compound would be more effective in a model that entrains both arms of the adaptive immune system. We therefore tested EDO-S101 in the EAV rat model, mimicking the clinical scenario by treating from a point when the disease was clinically evident 28 days after immunisation with MPO. We observed a significant reduction in anti-hMPO titre between vehicle and EDO-S101 treated rats at day 56 **(Fig. 3A)** as well as reduction in both haematuria and albuminuria **(Fig. 3B+C)**. EAV rats treated with EDO-S101 exhibited dramatically improved GN, with a reduction in crescent fraction from 6.1±1.7% to 0.2±0.1% ($p<0.005$, **Fig. 3D**). EDO-S101 significantly reduced lung haemorrhage severity **(Fig. 4)** and there was a significant correlation between anti-MPO titre and glomerular injury **(Supplemental Fig. 4A+B)**.

EDO-S101 increases monocyte and neutrophil fraction in mice and neutrophil fraction in rats

Having shown a beneficial effect of EDO-S101 in EAV, we went on to dissect the corresponding cellular correlates using flow cytometry. EDO-S101 induced moderate overall leukopenia **(Supplemental Fig. 5).** In the murine model, there was an increase in both monocyte and neutrophil

The International Society of Nephrology (http://www.isn-online.org/site/cms)

For Peer Review Only

fraction by day 7 in EDO-S101 treated mice, indicating a sparing of this cell type relative to other leukocytes **(Fig. 5A, C)**. The fraction of activated monocytes and neutrophils was unaffected by EDO-S101 **(Supplemental Fig. 6).** A similar relative increase in neutrophil fraction **(Fig. 5D)** was observed in EDO-S101 treated rats with EAV. Corresponding absolute neutrophil and monocyte counts are shown in **Supplemental Fig. 7.**

The dominant therapeutic cellular effect of EDO-S101 in EAV is on the lymphoid compartment

Given the positive therapeutic effect of EDO-S101 in EAV rats, we included an analysis of NK, B and T cell populations to define the selective effect of EDO-S101. We observed a reduction in NK cell count during the evolution of EAV which rebounded by day 56 (**Supplemental Fig. 8A**). Although there was no significant effect on NK cell fraction following treatment with EDO-S101 **(Fig. 6A)**, a substantial reduction in rat B-cells and T-cells was observed **(Fig. 6B+C and Supplemental Fig. 8B+C)**.

Treatment with EDO-S101 induces apoptosis in B cells and increases DNA damage in EAV tissue.

To address its mechanistic effects on the immune system, we investigated the effects of EDO-S101 compared with those of Bendamustine or Vorinostat on a Seraphina Burkitt Lymphoma (BL) cell line. EDO-S101 reduced B cell viability (as determined by MTT assay) and reduced proliferation (as determined by temporal cell count) **(Fig. 7A+B)**. EDO-S101 increased B cell sub-diploid cell fractions **(Fig. 7C),** cleaved poly (adp-ribose) polymerase (PARP) levels **(Fig. 7D)** and propidium iodide (PI) staining (**Fig. 7E-H)**. Further staining for P53 and PH2AX in spleen tissue from rats treated with EDO-S101 showed a clear induction of both DNA damage markers **(Fig. 7I-K)**. Upregulation of p53 was particularly evident in EDO-S101 treated rats **(Fig. 7M)**, with extension beyond the restricted white pulp staining observed in vehicle treated animals **(Fig. 7J)**. Taken together, these results indicate an increase in apoptosis in EDO-S101 treated B cells and in EAV spleen.

For Peer Review Only

DISCUSSION

Existing alkylating agent therapy for AAV is largely effective at inducing remission, but at the cost of side effects and subsequent risk of relapse when the treatment is stopped. We hypothesised that the effect of a low dose of the alkylating agent Bendamustine could be potentiated by disrupting the chromatin structure, thereby making the DNA more accessible to the drug. This was achieved by creating a hybrid compound with the HDACi Vorinostat and testing it in two well established rodent models of MPO-AAV. Although the bi-functional molecule was relatively ineffective in a passive murine model, it proved highly efficacious in a rat model of AAV induced by active immunisation with MPO, even when given after establishment of disease. In a first experimental investigation of circulating leukocyte populations in the EAV model, we showed that this therapeutic effect was accompanied by a reduction in circulating B and T cells. This strongly suggests that the primary beneficial effect was mediated through action on the adaptive immune system.

It has been shown that pan-HDACi, such as Vorinostat, increase H3 tail acetylation in transformed human cells[10]. We previously confirmed this activity for EDO-S101 in MM1S cell lines[6], providing first evidence that the compound indeed functions as a pan-HDACi. Additionally, in the current study, EDO-S101 induced hyperacetylation of the H3 tail at lysine residues K9, K14, K23 and K56 in extracts of HL60 cells, and demonstrated greater acetylation capacity than Bendamustine alone.

Upon further investigation in EAV spleen tissue, we observed induction by EDO-S101 of both pH2AX and, particularly, P53 (which extended well beyond the restricted white pulp staining observed in the vehicle), indicating increased DNA damage. On the one hand, EDO-S101 causes DNA injury via its alkylating function (pH2AX response), while on the other hand, it suppresses the homologous DNA

The International Society of Nephrology (http://www.isn-online.org/site/cms)

For Peer Review Only

repair response (p-ATR and p-ATM suppression). We hypothesise that this combined activity renders the compound more effective than a conventional alkylating agent, making it applicable in a variety of disease settings[6]. These findings were complemented by proliferation assays in human B cells. We observed an increase in PARP cleavage in B cells treated with EDO-S101 which indicates cellular disassembly and, thereby, an increase in apoptosis. Additionally, an increase in sub-diploid DNA in EDO-S101 treated cells is also indicative of apoptosis. Consistent with the cell count and MTT data, EDO-S101 was significantly more potent at inducing apoptosis compared to equimolar concentrations of Bendamustine and Vorinostat, suggesting that it is possible to obtain similar effects with markedly reduced exposure to Bendamustine.

To provide a mechanistic cellular basis for the activity of the drug, we performed detailed assessment of peripheral leukocyte populations for the first time in these models. We observed a large reduction in peripheral leukocyte count on day 1 in the murine model, but a very dramatic increase in the neutrophil component of these cells. This is consistent with prior work that shows a large increase in peripheral neutrophil count on day 1[11], and is likely to be primarily an LPS effect. As we did not include lymphocyte populations in the murine panel, we cannot determine the effect of LPS on these cell types. We suggest that the observed reduction in total leukocyte count in the murine model on day 1 is likely to be secondary to induction of acute lymphopenia, noting that lymphocytes are the dominant leukocyte type in mice. Prior work has demonstrated that infusion of LPS causes acute lymphopenia, with up to 80% reduction in absolute lymphocyte count[12]. It should also be noted that the healthy control (HC) mice were studied at a different time than the current experimental mice, which may also have contributed to the marked difference.

Contrary to the effect of cyclophosphamide and other alkylating agents, EDO-S101 increased the fraction of circulating monocytes and neutrophils at the point of peak murine disease (day 7), and neutrophil fraction at peak EAV disease in the rat (day 56). Part of this increase in cell fractions is almost certainly due to relative reduction in other leukocyte types, with little change in absolute cell

For Peer Review Only

counts. The exception to this was the failure of the monocyte fraction to increase in EAV during EDO-S101 treatment, reflected in the reduction in absolute monocyte count in the rat. The explanation for this difference in monocyte response between mouse and rat may be due to lingering effects from the LPS in the mouse that were not evident with the longer EAV time course. Although the dominant effect of EDO-S101 appears to be on lymphocytes, this reduction in circulating rat monocyte numbers may have contributed to a reduction in glomerular recruitment and severity of GN.

EDO-S101 reduced the absolute monocyte cell count (but not fraction) on day 1 in the mouse, without significantly affecting neutrophil count. Overall, neutrophils were relatively spared compared to other leukocyte populations in both rodent models, with a significant increase in circulating fraction by day 7 in mouse and day 56 in rat. Prior work in the murine model has demonstrated the importance of neutrophils in this condition[13]. This relative sparing of neutrophils may partially explain why, in the neutrophil-dependent murine model, the compound was ineffective in this model. Although we did not measure this directly, in addition to its impact on leukocyte count, the HDACi effect may have altered the neutrophil chromatin structure. Ciavatta et al have proposed epigenetic disruption of PR3 and MPO gene silencing as a potential mechanism of triggering autoimmunity in AAV patients[14,15]. Although it is unlikely that these epigenetic effects are at play in these rodent models, it is interesting to speculate that EDO-S101 may target similar epigenetic effects, representing an additional potential mechanism of action.

Previous clinical and preclinical studies have shown that EDO-S101 exerts potent therapeutic effects against haematological malignancies and works on the adaptive immune response[7,8,16-18]. Given its ability to suppress B and T cells effectively in preclinical studies, it seemed plausible that treatment with EDO-S101 may provide therapeutic effects in autoimmune disease, such as AAV. Indeed, in this study, we observed a striking depletion of B and T cells in the EAV model following EDO-S101 treatment, and a significant reduction in anti-hMPO antibodies in the EAV model.

The International Society of Nephrology (http://www.isn-online.org/site/cms)

For Peer Review Only

When considering limitations in this study, it important to note experimental differences between the rat and mouse models. For example, no absolute monocyte or neutrophil cell counts were performed in mice; these were calculated from total leukocyte counts. Additionally, we did not include analysis of lymphocyte populations (B, T and NK cells) in the murine panel as carried out in the rat study, although little therapeutic effect was observed in the mice. Furthermore, HC mice were studied separately from the experimental mice. Neither of these murine or rat models are satisfactory models of human ANCA vasculitis, not least because of the relatively mild disease phenotype in both. Nevertheless, it is worth highlighting that they reflect different aspects of AAV pathogenesis, thereby allowing us to study the effects of EDO-S101 on the innate and adaptive immune response. Another interesting aspect to consider would be further phenotyping of the p53/pH2AX-positive spleen cells to determine whether these are of B or T cell origin (e.g. via CD3 or CD19 staining). Our findings do not definitively exclude the possibility that the therapeutic effects simply occurred as a non-specific consequence of leukopenia. Vorinostat, being a pan-HDACi, would have wide ranging effects on many cell types. However, the clear dichotomy between the effects of EDO-S101 on innate and adaptive immune responses argues against this; a non-specific effect would be expected to impact most on the rapidly renewing neutrophil pool.

To conclude, we have demonstrated varying therapeutic effects of a novel alkylating HDACi fusion molecule, EDO-S101, in two contrasting models of MPO-ANCA vasculitis. Our data indicate a selective effect of EDO-S101 on the adaptive immune response resulting in amelioration of GN and lung haemorrhage in the EAV model. Given the induction of apoptosis in proliferating human B cells and the rat B cell depletion *in vivo*, we speculate that EDO-S101 may act on the autoreactive B cell pool. Further work is required to determine optimal dosing strategy, whether an orally active version can be developed, and to assess whether the bi-functional molecule can reduce infectious complications. The current data suggest that EDO-S101 is a promising novel agent for treatment of AAV and support the pursuit of these additional pre-clinical studies.

The International Society of Nephrology (http://www.isn-online.org/site/cms)

For Peer Review Only

For Peer Review Only

MATERIALS AND METHODS

Animals

MPO$^{-/-}$ mice (B6.129X1-MPO^{tm1Lus}/J) were purchased from Jackson Laboratories (Bar Harbor, Maine) and bred in-house. Female C57BL/6J mice (8-10 weeks old) were purchased from Harlan (Horst, The Netherlands). WKY rats were derived from the inbred colony of authors CDP and FT and bred by Charles River (Margate, UK). Equal numbers of male and female rats (6-weeks old) were used throughout the experiment in both treatment groups. A mouse xenograft model was used for investigating the DNA damaging effects of EDO-S101 in tumour tissue as previously described[6]. All experiments were approved by the local ethical committees and performed according to the guidelines described on the protection of animals used for scientific purposes at University Medical Centre Groningen, Trinity College Dublin and Mundipharma-EDO GmbH (EU Directive 2010/63). See supplemental materials and methods for further details.

Western Blotting

Cells were centrifuged at 10,000 g for 2 min, washed with PBS and lysed in ice-cold lysis buffer (140 mM NaCl, 10 mM EDTA, 10% glycerol, 1% Nonidet P-40, 20 mM Tris (pH 7.0), 1 µM pepstatin, 1 µg/ml aprotinin, 1 µg/ml leupeptin, 1 mM sodium orthovanadate). Western blots were probed with antibodies to p-ATR, p-ATM, Chk2, cleaved PARP Asp214 (Cell Signalling, Boston, MA) and β-Actin (Sigma-Aldrich).

Murine passive transfer vasculitis disease induction and treatment protocol

Male and female C57Bl/6J mice were randomly divided into 4 groups: vehicle pre-treated and sacrificed at day 1 or 7 (n=8/group) or EDO-S101 pre-treated and sacrificed at day 1 or 7 (n=8/group). Mice received EDO-S101 (25 mg/kg) or vehicle intravenously (i.v) one day before disease induction. On the next day, disease was induced via i.v. administration of 1.5 mg of anti-

The International Society of Nephrology (http://www.isn-online.org/site/cms)

For Peer Review Only

MPO IgG, followed by LPS administration i.p. (5 µg/g) 1 hour later (Escherichia coli, serotype O26:B6; Sigma-Aldrich). See supplemental materials and methods for further details on polyclonal mouse anti-MPO IgG production.

Urine and plasma analysis of murine samples

Urine samples were collected from mice at varying time points using metabolic cages. Haematuria was assessed with dipstick (score 0-4) at day 1-7 using Combur-Test strips (Roche Diagnostics BV, Netherlands). Albuminuria (day 1 and 7) was measured by ELISA (quantitation kit; Bethyl Laboratories, USA) following the manufacturer's instructions. Plasma samples were tested for circulating anti-MPO antibody titres by ELISA at days 1 and 7 as described above using a serum pool from MPO immunized MPO-/- mice for reference as previously described[21].

Flow cytometry of murine samples

Automated total and differential white blood cell counts (WBC) were determined at time of sacrifice (day 1 and 7) using the Sysmex XT-1800iV (Sysmex, The Netherlands). Neutrophils ($Ly6G^{+}CD11b^{high}$) and monocytes ($Ly6G^{-}CD11b^{+}$) and their activation status, were analysed in peripheral blood by Flow cytometry on a Calibur flow cytometer (BD BioSciences). See supplemental materials and methods for further details.

Experimental autoimmune vasculitis protocol

EAV, a model of MPO-ANCA vasculitis, was induced in male and female rats, as previously described[19]. Unimmunised animals were included to provide a comparison to the basal state. Co-housed rats were randomly divided into 2 groups: vehicle or EDO-S101 (10 mg/kg) treated (n=7-8/group) and received treatment intravenously into the lateral tail vein starting at day 28 (baseline), given that we have previously shown well-established disease at day 28 in this model[20]. All rats were sacrificed at day 56. See supplemental materials and methods for further details.

The International Society of Nephrology (http://www.isn-online.org/site/cms)

For Peer Review Only

Urine and plasma analysis of rat samples

Urine samples were collected from rats at day 56 using metabolic cages and haematuria was assessed with dipstick (score 0-4) using Multistix (Siemens, Ireland). Albuminuria was measured by ELISA (Nephrat kit; Exocell, USA), following the manufacturer's instructions. Plasma samples were tested for circulating anti-human (h)MPO antibody titres by ELISA at day 56 as previously described[19,21]. See supplemental materials and methods for further details.

Flow cytometry of rat samples

Peripheral blood was taken from healthy controls, rats on day 28 post immunisation (baseline disease) and at the time of sacrifice (day 56) and analysed by flow cytometry to determine leukocyte subsets. Samples were analysed on a CyAn ADP analyser (Beckman Coulter). Subsequent analysis was performed using Kaluza v1.2 analysis software (Beckman Coulter). Frequencies and absolute numbers of the following leukocyte subsets were determined as: total leukocytes ($CD45^+$), neutrophils ($SSC^{hi}RP\text{-}1^+$), monocytes ($CD3^-CD4^+$), B cells ($CD45RA^+$), T cells ($CD3^+$), NK cells ($CD3^-CD161a^+$). See supplemental materials and methods for further details.

Cell viability and analysis of DNA content in human B cells

Seraphina BL cells were treated as described in figure legends with DMSO control, EDO-S101, Bendamustine (Sigma-Aldrich) or Vorinostat (Sigma-Aldrich). After the indicated times, cells were harvested and counted. Cell viability was analysed via an MTT assay. Additionally, PI-stained cells were analysed for DNA content by flow cytometry using a CyAn ADP analyser (Beckman Coulter). See supplemental materials and methods for further details.

Immunohistopathological Analysis

Activation of p53 induces the expression of a variety of gene products, which can in turn either prevent proliferation of damaged cells, or induce apoptosis, thereby removing damaged cells from

The International Society of Nephrology (http://www.isn-online.org/site/cms)

For Peer Review Only

the body[22]. Phosphorylation of H2AX plays a major role in the DNA damage response and is required for the assembly of DNA repair proteins[23]. Therefore, we investigated these molecules given their role in apoptosis and DNA damage[9,23]. For analysis of the xenograft model, selected tumours excised from treated and control mice were stained for anti-pH2AX and anti-p53 (Cell Signaling, Boston, MA). To further investigate the effect of EDO-S101 on DNA damage, rat spleen sections (10µm) were also stained for anti-pH2AX and anti-p53 (Cell Signaling, Boston, MA). For analysis of the vasculitis models, kidney sections (4µm) were stained with periodic acid-Schiff (PAS) and haematoxylin and eosin (H&E) to assess morphology as previously described[19-21,24]. In addition to kidney pathology, rats with EAV develop pulmonary vasculitis and haemorrhage as previously described[25]. See supplemental materials and methods for further details.

Statistical Analysis

All statistical analyses were performed using GraphPad Prism 6.0 software. Mouse haematuria and albuminuria were analysed using two-way ANOVA, including time as a variable. All other comparisons between two groups were evaluated using the nonparametric Mann-Whitney U test. Differences were considered statistically significant when $p < 0.05$. Data represent mean values per experimental group ±SEM.

For Peer Review Only

FIGURE LEGENDS

Figure 1: Induction of global Histone 3 hyperacetylation and increased DNA damage of tumor tissue following treatment with EDO-S101.

(A) Hyperacetylation of Histone 3 (H3) and specific lysine residues in HL60 cells following treatment with EDO-S101 compared with Bendamustine (Bend). **(B)** p53 and pH2AX staining on *in vivo* tumor tissue from Daudi Burkitt's lymphoma on samples taken at day 4 and 8, showing greater DNA repair response after a single dose of 40 mg/kg or 80 mg/kg EDO-S101, compared with vehicle. **Scale bars = 100 µm.**

Figure 2: Pre-treatment with EDO-S101 in mice modestly decreases albuminuria but has no effect on glomerular histopathology.

(A) Anti-MPO antibody titres after induction of anti-MPO IgG/LPS-mediated GN in mice at days 1 and 7. **(B)** Albuminuria was significantly reduced in EDO-S101 pre-treated mice, compared with vehicle controls. **(C)** Quantification of crescentic glomeruli showed no significant differences between treatment groups. **(D-K)** Representative glomerular histology in vehicle and EDO-S101 pre-treated mice. **(D+E)** Necrotic glomerulus (Periodic acid-Schiff stain) on day 1 after disease induction in vehicle and EDO-S101 pre-treated mice respectively. **(F+G)** Neutrophil staining (Ly6G) 1 day after disease induction from vehicle and EDO-S101 pre-treated mice respectively. **(H+I)** Overview of renal cortical tissue (H&E stain) on day 7 after disease induction with a similar number of glomerular crescents in both vehicle and EDO-S101 pre-treated mice (red arrows). **(J+K)** Crescentic glomeruli (H&E stain) in vehicle and EDO-S101 pre-treated mice respectively on day 7 after disease induction. Data represents mean ± SEM; *p<0.05. **Scale bars: D-G, J+K = 50 µm, H+I = 100 µm.**

Figure 3: EDO-S101 treatment in rats significantly decreases both haematuria and albuminuria and ameliorates proliferative and crescentic glomerulonephritis.

The International Society of Nephrology (http://www.isn-online.org/site/cms)

For Peer Review Only

(A) Anti-hMPO antibody titres at day 56 days after induction of EAV in rats. Treatment with EDO-S101 in EAV rats led to significantly reduced **(B)** haematuria **(C)** albuminuria and **(D)** Crescentic GN compared with vehicle treated controls at day 56. **(E-L)** Representative glomerular histology in vehicle and EDO-S101 treated rats. **(E)** Foci of interstitial infiltrates and red cell tubular casts (H&E stain; red arrows) in vehicle and **(F)** mild interstitial infiltrates in EDO-S101 treated rats. **(G)** Mild GN, intense peri-glomerular inflammation and red cell casts (H&E stain; red arrows) in vehicle-treated rats. **(H)** Focus on inflammatory tubular destruction in EDO-S101 treated rats (H&E). **(I+K)** Crescentic GN in vehicle treated rats with intense peri-glomerular inflammation and red cell casts (PAS stain; red arrows). **(J)** Mild GN in EDO-S101 treated rats with **(L)** focal glomerular necrosis and early crescent formation (PAS stain; red arrows). Data represents mean ± SEM; *p<0.05, **p<0.01. **Scale bars: E+F = 500 µm, G = 200 µm, H-J = 100 µm, K+L = 50 µm.**

Figure 4: Treatment with EDO-S101 significantly decreases lung haemorrhage in EAV rats.

(A+B) The macroscopic lung petechiae score was determined by assessment of the right lung of **(A)** vehicle and **(B)** EDO-S101 treated animals; lung haemorrhages highlighted by white arrows **(C+D)** Antemortem lung haemorrhage shown by the presence of Perl's positive cells (blue, red arrow) in the lungs of **(C)** vehicle and **(D)** EDO-S101 treated rats. Alveolar hypocellularity of **(E, G)** vehicle treated animals, with thickening of alveolar walls (arrow). EDO-S101 treated rats **(F, H)** had minimal alveolar wall thickening (H&E, 100 and 400X). **(I)** Lung petechiae score of vehicle and EDO-S101 treated rats. Data represents mean; *p<0.05. **Scale bars: C+D, G+H = 50 µm, E+F = 100 µm.**

Figure 5: Impact of treatment with EDO-S101 on relative myeloid cell fractions.

(A) Pre-treatment with EDO-S101 in mice significantly increased the percentage of monocytes from leukocytes at day 7. **(B)** In rats, treatment with EDO-S101 had no significant effect on the percentage of monocytes from leukocytes at day 56. **(C)** Pre-treatment with EDO-S101 in mice significantly increased the percentage of neutrophils from leukocytes at day 7. **(D)** In rats, treatment with EDO-

The International Society of Nephrology (http://www.isn-online.org/site/cms)

For Peer Review Only

S101 increased the percentage of neutrophils from leukocytes compared to vehicle controls. HC represents unimmunised healthy controls, while BL denotes baseline disease in rats (day 28 post-immunisation). Data represents mean ± SEM; ***p<0.001.

Figure 6: Treatment with EDO-S101 results in selective depletion of B cells and T cells in rats compared with vehicle treated controls.

(A) There was a non-significant trend towards a decrease in the percentage of NK cells from leukocytes compared with vehicle treated controls. There was a significant decrease in **(B)** B cell and **(C)** T cell percentages from leukocytes following treatment with EDO-S101 compared with vehicle treated controls. HC represents unimmunised healthy controls, while BL denotes baseline disease in rats (day 28 post-immunisation). Data represents mean ± SEM; **p<0.01, ***p<0.001.

Figure 7: Treatment with EDO-S101 induces apoptosis in a B cell line and increases DNA damage in EAV tissue.

(A) Seraphina BL cells were cultured at 1 x 10^6 cells/ml in the presence of increasing concentrations of EDO-S101, Bendamustine or Vorinostat, and viability of cells was assessed by MTT assay 16 hours later. Viability assessed at 6 hours is shown in Supplemental figure 9. **(B)** BL Cells were cultured in 25µM EDO-S101, Bendamustine or Vorinostat and cells were counted at indicated time points. **(C)** Percentage sub-diploid cells was measured from DNA content of treated cells. **(D)** BL cells were cultured in 25µM EDO-S101, Bendamustine or Vorinostat and harvested at the indicated time points then probed for levels of cleaved PARP (Asp 214). **(E-H)** Representative histograms of 16 hour treated cells, fixed and stained with PI for DNA content analysis. Representative photomicrographs of spleen tissue from **(I-K)** vehicle and **(L-N)** EDO-S101 treated rats stained for P53 and PH2AX are indicated. There is a clear induction of both markers in EDO-S101 treated rats, particularly **(M)** P53, which extends beyond the restricted white pulp staining observed in **(J)** vehicle treated animals. Error bars represent mean ± SEM; ***p<0.001. **Scale bars: I-N = 50 µm.**

For Peer Review Only

REFERENCES

1. Kallenberg CGM. Pathogenesis of ANCA-associated vasculitides. *Annals of the Rheumatic Diseases.* 2011;70(Suppl 1):i59-i63.
2. Jennette JC, Falk RJ. Pathogenesis of antineutrophil cytoplasmic autoantibody-mediated disease. *Nat Rev Rheumatol.* 2014;10(8):463-473.
3. Tesar V, Hruskova Z. Limitations of Standard Immunosuppressive Treatment in ANCA-Associated Vasculitis and Lupus Nephritis. *Nephron Clinical Practice.* 2014;128(3-4):205-215.
4. Frew AJ, Johnstone RW, Bolden JE. Enhancing the apoptotic and therapeutic effects of HDAC inhibitors. *Cancer Letters.* 2009;280(2):125-133.
5. Hancock WW, Akimova T, Beier UH, Liu Y, Wang L. HDAC inhibitor therapy in autoimmunity and transplantation. *Annals of the Rheumatic Diseases.* 2012;71(Suppl 2):i46-i54.
6. Mehrling T, Chen Y. The Alkylating-HDAC Inhibition Fusion Principle: Taking Chemotherapy to the Next Level with the First in Class Molecule EDO-S101. *Anti-Cancer Agents in Medicinal Chemistry.* 2016;16(1):20-28.
7. López-Iglesias AA, San-Segundo L, González-Méndez L, et al. The Alkylating Histone Deacetylase Inhibitor Fusion Molecule Edo-S101 Displays Full Bi-Functional Properties in Preclinical Models of Hematological Malignancies. *Blood.* 2014;124(21):2100-2100.
8. Kraus M, Bader J, Mehrling T, Driessen C. Edo- S101, a New Alkylating Histone-Deacetylase Inhibitor (HDACi) Fusion Molecule, Has Superior Activity Against Myeloma and B Cell Lymphoma and Strong Synergy with Proteasome Inhibitors in Vitro. *Blood.* 2014;124(21):2249-2249.
9. Di Benedetto A, Ercolani C, Mottolese M, et al. Analysis of the ATR-Chk1 and ATM-Chk2 pathways in male breast cancer revealed the prognostic significance of ATR expression. *Scientific Reports.* 2017;7(1):8078.
10. Drogaris P, Villeneuve V, Pomiès C, et al. Histone Deacetylase Inhibitors Globally Enhance H3/H4 Tail Acetylation Without Affecting H3 Lysine 56 Acetylation. *Scientific Reports.* 2012;2:220.
11. Wang Q, van Timmeren MM, Petersen AH, et al. Age-determined severity of anti-myeloperoxidase autoantibody-mediated glomerulonephritis in mice. *Nephrology Dialysis Transplantation.* 2017;32(2):254-264.
12. Copeland S, Warren HS, Lowry SF, et al. Acute Inflammatory Response to Endotoxin in Mice and Humans. *Clinical and Diagnostic Laboratory Immunology.* 2005;12(1):60-67.
13. Xiao H, Heeringa P, Liu Z, et al. The Role of Neutrophils in the Induction of Glomerulonephritis by Anti-Myeloperoxidase Antibodies. *The American Journal of Pathology.* 2005;167(1):39-45.
14. Ciavatta DJ, Yang J, Preston GA, et al. Epigenetic basis for aberrant upregulation of autoantigen genes in humans with ANCA vasculitis. *J Clin Invest.* 2010;120(9):3209-3219.
15. McInnis EA, Badhwar AK, Muthigi A, et al. Dysregulation of autoantigen genes in ANCA-associated vasculitis involves alternative transcripts and new protein synthesis. *J Am Soc Nephrol.* 2015;26(2):390-399.
16. Besse L, Kraus M, Besse A, Bader J, Mehrling T, Driessen C. The First in Class, Alkylator-Histone-Deacetylase-Inhibitor Fusion Molecule Edo-S101 in Combination with Proteasome Inhibitors Induces Highly Synergistic Pro-Apoptotic Signaling through UPR Activation and Suppression of c-Myc and BCL2 in Multiple Myeloma. *Blood.* 2016;128(22):4466-4466.
17. De Filippi R, Crisci S, Cillo M, et al. The First-in-Class Alkylating Histone-Deacetylase Inhibitor (HDACi) Fusion Molecule Edo-S101 Exerts Potent Preclinical Activity Against Tumor Cells of Hodgkin Lymphoma (HL) Including Bendamustine-Resistant Clones. *Blood.* 2015;126(23):2481-2481.

For Peer Review Only

18. López-Iglesias AA, Herrero AB, San-Segundo L, et al. The Hybrid Molecule, Edo-S101, Impairs Double Strand Breaks Repair in Multiple Myeloma and Synergizes with Bortezomib and Dexamethasone. *Blood.* 2015;126(23):5354-5354.
19. Little MA, Smyth L, Salama AD, et al. Experimental Autoimmune Vasculitis : An Animal Model of Anti-neutrophil Cytoplasmic Autoantibody-Associated Systemic Vasculitis. *The American Journal of Pathology.* 2009;174(4):1212-1220.
20. O'Reilly VP, Wong L, Kennedy C, et al. Urinary Soluble CD163 in Active Renal Vasculitis. *Journal of the American Society of Nephrology.* 2016.
21. Little MA, Bhangal G, Smyth CL, et al. Therapeutic Effect of Anti–TNF-α Antibodies in an Experimental Model of Anti-Neutrophil Cytoplasm Antibody–Associated Systemic Vasculitis. *Journal of the American Society of Nephrology.* 2006;17(1):160-169.
22. Caspari T. Checkpoints: How to activate p53. *Current Biology.* 2000;10(8):R315-R317.
23. Podhorecka M, Skladanowski A, Bozko P. H2AX Phosphorylation: Its Role in DNA Damage Response and Cancer Therapy. *Journal of Nucleic Acids.* 2010;2010:9.
24. Xiao H, Heeringa P, Hu P, et al. Antineutrophil cytoplasmic autoantibodies specific for myeloperoxidase cause glomerulonephritis and vasculitis in mice. *The Journal of Clinical Investigation.* 2002;110(7):955-963.
25. Al-Ani B, Fitzpatrick M, Al-Nuaimi H, et al. Changes in urinary metabolomic profile during relapsing renal vasculitis. *Scientific Reports.* 2016;6:38074.

For Peer Review Only

AUTHOR CONTRIBUTIONS

DD participated in collection and/or assembly of data, data analysis/interpretation, and manuscript writing. MMvT, VOR and EOB participated in the study design and data analysis/interpretation. GB, BF, FH, EL, CP and FT participated in the data analysis/interpretation and manuscript writing. TH, PH and ML participated in the study design, conception and coordination and helped to draft the final manuscript. All authors read and approved the final manuscript.

ACKNOWLEDGEMENTS

This study was supported by Science Foundation Ireland grant 11/Y/B2093. FWKT is supported by the Diamond Fund from Imperial College Healthcare Charity and Ken and Mary Minton Chair of Renal Medicine.

DISCLOSURE

TM is an employee of Mundipharma-EDO GmbH. FWKT has received research project grants from AstraZeneca Limited, Baxter Biosciences, Boehringer Ingelheim, and MedImmune, and has consultancy agreements with Rigel Pharmaceuticals, Novartis and Baxter Biosciences. CDP has received a research project grant from GlaxoSmithKline. The experimental work was funded by Mundipharma.

For Peer Review Only

ORIGINAL ARTICLE

Title: Alkylating Histone Deacetylase Inhibitor treatment in experimental MPO-ANCA Vasculitis

Running Title: Alkylating HDACi treatment in MPO-ANCA Vasculitis

Authors: Dearbhaile Dooley; PhD[1], Mirjan M van Timmeren[2]; PhD[2], Vincent P. O'Reilly; PhD[1], Gareth Brady; PhD[1], Eóin C. O'Brien; PhD[1], Barbara Fazekas; PhD[1], Fionnuala B. Hickey; PhD[1], Emma Leacy; BSc[1], Charles D. Pusey; PhD[3], Frederick W. K. Tam; PhD[3], Thomas Mehrling; PhD[4], Peter Heeringa; PhD[2], Mark A. Little; PhD[1,5 *]

Author affiliations

[1]Trinity Health Kidney Centre, Trinity Translational Medicine Institute, Trinity College Dublin, St. James' Hospital Campus, Ireland

[2]Department of Pathology and Medical Biology, University of Groningen, University Medical Centre Groningen, Groningen, The Netherlands

[3]Renal and Vascular Inflammation Section, Department of Medicine, Imperial College London, United Kingdom

[4]Mundipharma-EDO GmbH, Basel, Switzerland

[5]Irish Centre for Vascular Biology, Trinity College Dublin, Ireland

*Corresponding author

Prof. Mark A. Little

Trinity Health Kidney Centre, Trinity Translational Medicine Institute, Trinity College Dublin, St. James' Hospital Campus, Dublin 8, Ireland

Phone: +353 1896 3706

Email: mlittle@tcd.ie

Word count = 4002

For Peer Review Only

ABSTRACT

Current therapies for treating anti-neutrophil cytoplasm autoantibody (ANCA)-associated vasculitis include cyclophosphamide and corticosteroids. Despite inducing remission in most patients, these agents are associated with severe adverse effects. Histone deacetylase inhibitors (HDACi) are effective in rodent models of inflammation and act synergistically with many pharmacological agents, including alkylating agents like cyclophosphamide. EDO-S101 is an alkylating HDACi fusion molecule combining the DNA alkylating effect of Bendamustine, with a pan-HDACi, Vorinostat. We studied the effects of EDO-S101 in two established rodent models of ANCA-associated vasculitis: a passive mouse model of anti-myeloperoxidase IgG-induced glomerulonephritis and an active rat model of anti-myeloperoxidase-ANCA microscopic polyangiitis (EAV). Although pre-treatment with EDO-S101 reduced circulating leukocytes, it did not prevent development of passive IgG-induced glomerulonephritis in mice. On the other hand, treatment in rats significantly reduced glomerulonephritis and lung haemorrhage. EDO-S101 also significantly depleted rat B and T cells, and induced DNA damage and apoptosis in proliferating human B cells, suggesting a selective effect on the adaptive immune response. Taken together, EDO-S101 may have a role in treatment of ANCA-associated vasculitis, operating primarily through its effects on the adaptive immune response to the autoantigen myeloperoxidase.

For Peer Review Only

INTRODUCTION

Anti-neutrophil cytoplasm autoantibody (ANCA)-associated vasculitis (AAV) is a systemic autoimmune condition that affects small- to medium-sized blood vessels. Severe vessel wall damage causes inflammatory necrosis and consequent loss of organ function. The lungs and kidneys are frequently affected, leading to lung haemorrhage and glomerulonephritis (GN). Patients with AAV develop circulating autoantibodies against the neutrophil granule and monocyte lysosomal enzymes myeloperoxidase (MPO) or proteinase 3 (PR3)[1,2]. Conventional treatment includes cyclophosphamide and corticosteroids, which induces remission in most patients. However, these therapies do not fully prevent disease relapse and patients often require long-term treatment, which is associated with severe morbidity[3]. This highlights the urgent need for development of new therapies.

Histone deacetylase inhibitors (HDACi) were originally described as a class of anti-cancer drugs in 2006 due to their growth arrest and apoptotic effects on tumour cells[4]. They target the histone deacetylase enzymes which remove the acetyl groups from lysine residues, leading to chromatin condensation and transcriptional silencing. HDACi thus result in histone hyperacetylation, thereby affecting gene transcription. This enhances activity of some transcription factors such as the tumour suppressor p53, but represses B and T-cell transcription factors. Therefore, in the setting of autoimmunity, HDACi can induce cell cycle arrest or apoptosis of key leukocyte populations that are proliferating in response to auto-antigen exposure. Recently, HDACi were shown to have beneficial effects in inflammatory rodent models, such as arthritis, asthma and colitis; however, their mechanism(s) of action are not well understood[5]. HDACi act synergistically with a diverse range of pharmacological and biological agents, including cyclophosphamide. Therefore, it appears likely that HDACi may be best used in the clinic as part of a combination regimen, enabling a multitarget approach.

For Peer Review Only

EDO-S101, a small molecule compound developed by Mundipharma GmbH, is an alkylating HDACi fusion molecule which combines the strong DNA damaging effect of Bendamustine, with a fully functional pan-HDACi, Vorinostat. This combination therapy has the potential to provide enhanced efficacy at a lower alkylating agent dose due to its bi-functional mode of action. HDAC inhibition allows for better access of the alkylating moiety to the DNA double strands by opening the chromatin, thereby creating the potential for enhanced synergy between the two moieties. EDO-S101 has demonstrated good tolerability and exerts significant activity against haematological malignancy and solid tumours[6-8].

We hypothesised that EDO-S101 is an effective therapy for AAV. To dissect its effects on both the innate and adaptive immune response, we tested its efficacy in two well established rodent models of MPO-AAV: a passive mouse model of anti-MPO IgG-induced GN and an active rat model of Experimental Autoimmune Vasculitis (EAV). EAV is an MPO-ANCA vasculitis model induced by immunisation of Wistar Kyoto (WKY) rats with hMPO, resulting in crescentic GN and lung haemorrhage. These features of mild pauci-immune vasculitis are indistinguishable pathologically from human vasculitis, making EAV a valuable pre-clinical model in AAV. We observed that EDO-S101 was largely ineffective in the murine model but dramatically improved renal and lung disease in the rat model. Thus, EDO-S101 shows potential as a novel treatment for AAV, largely through its action on the adaptive immune response.

For Peer Review Only

RESULTS

EDO-S101 induces global H3 hyperacetylation in HL60 Cells and a strong DNA repair response *in vivo*

Hyperacetylation of the Histone3 (H3) tail at lysine residues K9, K14, K23 and K56 was measured using specific antibodies for acetylated lysine residues in total cell extracts of HL60 cells **(Fig. 1A).** EDO-S101 demonstrated enhanced acetylation of lysine residues, whereas Bendamustine (Bend) was equivalent to the DMSO control **(Fig. 1A)**. Exposure to EDO-S101 *in vivo* caused a strong DNA repair response (activation of p53 and pH2AX) in tumours taken at day 4 and 8 from mice bearing subcutaneous human Daudi Burkitt's lymphoma **(Fig. 1B).** Both ataxia telangiectasia mutated (ATM) kinase and Rad3-related protein (ATR) are activated upon DNA damage. Following their recruitment to DNA damage sites, ATM and ATR activate the Checkpoint Kinase 2 (Chk2) and Checkpoint kinase 1 (Chk1), respectively. These kinases were investigated as their pathways are central in DNA damage repair and their over-activation may confer aggressive molecular features, including endogenous DNA damage and oncogene-induced replication stress[9]. Taken together, these allowed us to investigate the simultaneous effects of EDO-S101 on DNA damage and blocking of damage repair. Indirect HDACi activity was measured in tumour samples on days 4 and 8; p-ATR and p-ATM were dose dependently suppressed by EDO-S101 treatment. On the other hand, p-CHK2 was strongly upregulated at day 4, but returned to undetectable levels at day 8 **(Supplemental Fig. 1A)**.

EDO-S101 has little effect on anti-MPO induced vasculitis in a passive transfer model of MPO-AAV

Given the potent combination of HDACi and alkylating capacity of the compound, we tested the ability of EDO-S101 to prevent vasculitic injury induced by anti-MPO antibodies in a passive transfer

The International Society of Nephrology (http://www.isn-online.org/site/cms)

For Peer Review Only

model, with the compound given from the time of antibody transfer. Circulating anti-MPO antibody levels were similar in vehicle and EDO-S101 pre-treated mice at day 1 and day 7 **(Fig. 2A and Supplemental Fig. 2A).** Following disease induction, both vehicle and EDO-S101 pre-treated mice developed characteristic haematuria, which decreased over time (day 1 to day 7). Although there was no significant effect on haematuria **(Supplemental Fig. 2B),** EDO-S101 reduced albuminuria compared with vehicle treated controls **(Fig. 2B)**. Both vehicle and EDO-S101 pre-treated mice developed GN **(Fig. 2D-K)**, with no significant effect of EDO-S101 on crescentic GN **(Fig. 2C)** or glomerular histopathology evident **(Supplemental Fig. 3A+B)**.

Treatment of the active model of EAV with EDO-S101 abolishes crescentic glomerulonephritis and reduces lung haemorrhage

As there was little impact of EDO-S101 on a direct antibody-induced model of vasculitis, we hypothesised that the compound would be more effective in a model that entrains both arms of the adaptive immune system. We therefore tested EDO-S101 in the EAV rat model, mimicking the clinical scenario by treating from a point when the disease was clinically evident 28 days after immunisation with MPO. We observed a significant reduction in anti-hMPO titre between vehicle and EDO-S101 treated rats at day 56 **(Fig. 3A)** as well as reduction in both haematuria and albuminuria **(Fig. 3B+C)**. EAV rats treated with EDO-S101 exhibited dramatically improved GN, with a reduction in crescent fraction from 6.1±1.7% to 0.2±0.1% ($p<0.005$, **Fig. 3D**). EDO-S101 significantly reduced lung haemorrhage severity **(Fig. 4)** and there was a significant correlation between anti-MPO titre and glomerular injury **(Supplemental Fig. 4A+B)**.

EDO-S101 increases monocyte and neutrophil fraction in mice and neutrophil fraction in rats

Having shown a beneficial effect of EDO-S101 in EAV, we went on to dissect the corresponding cellular correlates using flow cytometry. EDO-S101 induced moderate overall leukopenia **(Supplemental Fig. 5).** In the murine model, there was an increase in both monocyte and neutrophil

The International Society of Nephrology (http://www.isn-online.org/site/cms)

For Peer Review Only

fraction by day 7 in EDO-S101 treated mice, indicating a sparing of this cell type relative to other leukocytes **(Fig. 5A, C)**. The fraction of activated monocytes and neutrophils was unaffected by EDO-S101 **(Supplemental Fig. 6).** A similar relative increase in neutrophil fraction **(Fig. 5D)** was observed in EDO-S101 treated rats with EAV. Corresponding absolute neutrophil and monocyte counts are shown in **Supplemental Fig. 7.**

The dominant therapeutic cellular effect of EDO-S101 in EAV is on the lymphoid compartment

Given the positive therapeutic effect of EDO-S101 in EAV rats, we included an analysis of NK, B and T cell populations to define the selective effect of EDO-S101. We observed a reduction in NK cell count during the evolution of EAV which rebounded by day 56 (**Supplemental Fig. 8A**). Although there was no significant effect on NK cell fraction following treatment with EDO-S101 **(Fig. 6A)**, a substantial reduction in rat B-cells and T-cells was observed **(Fig. 6B+C and Supplemental Fig. 8B+C)**.

Treatment with EDO-S101 induces apoptosis in B cells and increases DNA damage in EAV tissue.

To address its mechanistic effects on the immune system, we investigated the effects of EDO-S101 compared with those of Bendamustine or Vorinostat on a Seraphina Burkitt Lymphoma (BL) cell line. EDO-S101 reduced B cell viability (as determined by MTT assay) and reduced proliferation (as determined by temporal cell count) **(Fig. 7A+B)**. EDO-S101 increased B cell sub-diploid cell fractions **(Fig. 7C),** cleaved poly (adp-ribose) polymerase (PARP) levels **(Fig. 7D)** and propidium iodide (PI) staining (**Fig. 7E-H)**. Further staining for P53 and PH2AX in spleen tissue from rats treated with EDO-S101 showed a clear induction of both DNA damage markers **(Fig. 7I-K)**. Upregulation of p53 was particularly evident in EDO-S101 treated rats **(Fig. 7M)**, with extension beyond the restricted white pulp staining observed in vehicle treated animals **(Fig. 7J)**. Taken together, these results indicate an increase in apoptosis in EDO-S101 treated B cells and in EAV spleen.

For Peer Review Only

DISCUSSION

Existing alkylating agent therapy for AAV is largely effective at inducing remission, but at the cost of side effects and subsequent risk of relapse when the treatment is stopped. We hypothesised that the effect of a low dose of the alkylating agent Bendamustine could be potentiated by disrupting the chromatin structure, thereby making the DNA more accessible to the drug. This was achieved by creating a hybrid compound with the HDACi Vorinostat and testing it in two well established rodent models of MPO-AAV. Although the bi-functional molecule was relatively ineffective in a passive murine model, it proved highly efficacious in a rat model of AAV induced by active immunisation with MPO, even when given after establishment of disease. In a first experimental investigation of circulating leukocyte populations in the EAV model, we showed that this therapeutic effect was accompanied by a reduction in circulating B and T cells. This strongly suggests that the primary beneficial effect was mediated through action on the adaptive immune system.

It has been shown that pan-HDACi, such as Vorinostat, increase H3 tail acetylation in transformed human cells[10]. We previously confirmed this activity for EDO-S101 in MM1S cell lines[6], providing first evidence that the compound indeed functions as a pan-HDACi. Additionally, in the current study, EDO-S101 induced hyperacetylation of the H3 tail at lysine residues K9, K14, K23 and K56 in extracts of HL60 cells, and demonstrated greater acetylation capacity than Bendamustine alone.

Upon further investigation in EAV spleen tissue, we observed induction by EDO-S101 of both pH2AX and, particularly, P53 (which extended well beyond the restricted white pulp staining observed in the vehicle), indicating increased DNA damage. On the one hand, EDO-S101 causes DNA injury via its alkylating function (pH2AX response), while on the other hand, it suppresses the homologous DNA

The International Society of Nephrology (http://www.isn-online.org/site/cms)

For Peer Review Only

repair response (p-ATR and p-ATM suppression). We hypothesise that this combined activity renders the compound more effective than a conventional alkylating agent, making it applicable in a variety of disease settings[6]. These findings were complemented by proliferation assays in human B cells. We observed an increase in PARP cleavage in B cells treated with EDO-S101 which indicates cellular disassembly and, thereby, an increase in apoptosis. Additionally, an increase in sub-diploid DNA in EDO-S101 treated cells is also indicative of apoptosis. Consistent with the cell count and MTT data, EDO-S101 was significantly more potent at inducing apoptosis compared to equimolar concentrations of Bendamustine and Vorinostat, suggesting that it is possible to obtain similar effects with markedly reduced exposure to Bendamustine.

To provide a mechanistic cellular basis for the activity of the drug, we performed detailed assessment of peripheral leukocyte populations for the first time in these models. We observed a large reduction in peripheral leukocyte count on day 1 in the murine model, but a very dramatic increase in the neutrophil component of these cells. This is consistent with prior work that shows a large increase in peripheral neutrophil count on day 1[11], and is likely to be primarily an LPS effect. As we did not include lymphocyte populations in the murine panel, we cannot determine the effect of LPS on these cell types. We suggest that the observed reduction in total leukocyte count in the murine model on day 1 is likely to be secondary to induction of acute lymphopenia, noting that lymphocytes are the dominant leukocyte type in mice. Prior work has demonstrated that infusion of LPS causes acute lymphopenia, with up to 80% reduction in absolute lymphocyte count[12]. It should also be noted that the healthy control (HC) mice were studied at a different time than the current experimental mice, which may also have contributed to the marked difference.

Contrary to the effect of cyclophosphamide and other alkylating agents, EDO-S101 increased the fraction of circulating monocytes and neutrophils at the point of peak murine disease (day 7), and neutrophil fraction at peak EAV disease in the rat (day 56). Part of this increase in cell fractions is almost certainly due to relative reduction in other leukocyte types, with little change in absolute cell

The International Society of Nephrology (http://www.isn-online.org/site/cms)

For Peer Review Only

counts. The exception to this was the failure of the monocyte fraction to increase in EAV during EDO-S101 treatment, reflected in the reduction in absolute monocyte count in the rat. The explanation for this difference in monocyte response between mouse and rat may be due to lingering effects from the LPS in the mouse that were not evident with the longer EAV time course. Although the dominant effect of EDO-S101 appears to be on lymphocytes, this reduction in circulating rat monocyte numbers may have contributed to a reduction in glomerular recruitment and severity of GN.

EDO-S101 reduced the absolute monocyte cell count (but not fraction) on day 1 in the mouse, without significantly affecting neutrophil count. Overall, neutrophils were relatively spared compared to other leukocyte populations in both rodent models, with a significant increase in circulating fraction by day 7 in mouse and day 56 in rat. Prior work in the murine model has demonstrated the importance of neutrophils in this condition[13]. This relative sparing of neutrophils may partially explain why, in the neutrophil-dependent murine model, the compound was ineffective in this model. Although we did not measure this directly, in addition to its impact on leukocyte count, the HDACi effect may have altered the neutrophil chromatin structure. Ciavatta et al have proposed epigenetic disruption of PR3 and MPO gene silencing as a potential mechanism of triggering autoimmunity in AAV patients[14,15]. Although it is unlikely that these epigenetic effects are at play in these rodent models, it is interesting to speculate that EDO-S101 may target similar epigenetic effects, representing an additional potential mechanism of action.

Previous clinical and preclinical studies have shown that EDO-S101 exerts potent therapeutic effects against haematological malignancies and works on the adaptive immune response[7,8,16-18]. Given its ability to suppress B and T cells effectively in preclinical studies, it seemed plausible that treatment with EDO-S101 may provide therapeutic effects in autoimmune disease, such as AAV. Indeed, in this study, we observed a striking depletion of B and T cells in the EAV model following EDO-S101 treatment, and a significant reduction in anti-hMPO antibodies in the EAV model.

The International Society of Nephrology (http://www.isn-online.org/site/cms)

For Peer Review Only

When considering limitations in this study, it important to note experimental differences between the rat and mouse models. For example, no absolute monocyte or neutrophil cell counts were performed in mice; these were calculated from total leukocyte counts. Additionally, we did not include analysis of lymphocyte populations (B, T and NK cells) in the murine panel as carried out in the rat study, although little therapeutic effect was observed in the mice. Furthermore, HC mice were studied separately from the experimental mice. Neither of these murine or rat models are satisfactory models of human ANCA vasculitis, not least because of the relatively mild disease phenotype in both. Nevertheless, it is worth highlighting that they reflect different aspects of AAV pathogenesis, thereby allowing us to study the effects of EDO-S101 on the innate and adaptive immune response. Another interesting aspect to consider would be further phenotyping of the p53/pH2AX-positive spleen cells to determine whether these are of B or T cell origin (e.g. via CD3 or CD19 staining). Our findings do not definitively exclude the possibility that the therapeutic effects simply occurred as a non-specific consequence of leukopenia. Vorinostat, being a pan-HDACi, would have wide ranging effects on many cell types. However, the clear dichotomy between the effects of EDO-S101 on innate and adaptive immune responses argues against this; a non-specific effect would be expected to impact most on the rapidly renewing neutrophil pool.

To conclude, we have demonstrated varying therapeutic effects of a novel alkylating HDACi fusion molecule, EDO-S101, in two contrasting models of MPO-ANCA vasculitis. Our data indicate a selective effect of EDO-S101 on the adaptive immune response resulting in amelioration of GN and lung haemorrhage in the EAV model. Given the induction of apoptosis in proliferating human B cells and the rat B cell depletion *in vivo*, we speculate that EDO-S101 may act on the autoreactive B cell pool. Further work is required to determine optimal dosing strategy, whether an orally active version can be developed, and to assess whether the bi-functional molecule can reduce infectious complications. The current data suggest that EDO-S101 is a promising novel agent for treatment of AAV and support the pursuit of these additional pre-clinical studies.

The International Society of Nephrology (http://www.isn-online.org/site/cms)

For Peer Review Only

For Peer Review Only

MATERIALS AND METHODS

Animals

MPO$^{-/-}$ mice (B6.129X1-MPO^{tm1Lus}/J) were purchased from Jackson Laboratories (Bar Harbor, Maine) and bred in-house. Female C57BL/6J mice (8-10 weeks old) were purchased from Harlan (Horst, The Netherlands). WKY rats were derived from the inbred colony of authors CDP and FT and bred by Charles River (Margate, UK). Equal numbers of male and female rats (6-weeks old) were used throughout the experiment in both treatment groups. A mouse xenograft model was used for investigating the DNA damaging effects of EDO-S101 in tumour tissue as previously described[6]. All experiments were approved by the local ethical committees and performed according to the guidelines described on the protection of animals used for scientific purposes at University Medical Centre Groningen, Trinity College Dublin and Mundipharma-EDO GmbH (EU Directive 2010/63). See supplemental materials and methods for further details.

Western Blotting

Cells were centrifuged at 10,000 g for 2 min, washed with PBS and lysed in ice-cold lysis buffer (140 mM NaCl, 10 mM EDTA, 10% glycerol, 1% Nonidet P-40, 20 mM Tris (pH 7.0), 1 µM pepstatin, 1 µg/ml aprotinin, 1 µg/ml leupeptin, 1 mM sodium orthovanadate). Western blots were probed with antibodies to p-ATR, p-ATM, Chk2, cleaved PARP Asp214 (Cell Signalling, Boston, MA) and β-Actin (Sigma-Aldrich).

Murine passive transfer vasculitis disease induction and treatment protocol

Male and female C57Bl/6J mice were randomly divided into 4 groups: vehicle pre-treated and sacrificed at day 1 or 7 (n=8/group) or EDO-S101 pre-treated and sacrificed at day 1 or 7 (n=8/group). Mice received EDO-S101 (25 mg/kg) or vehicle intravenously (i.v) one day before disease induction. On the next day, disease was induced via i.v. administration of 1.5 mg of anti-

The International Society of Nephrology (http://www.isn-online.org/site/cms)

For Peer Review Only

MPO IgG, followed by LPS administration i.p. (5 µg/g) 1 hour later (Escherichia coli, serotype O26:B6; Sigma-Aldrich). See supplemental materials and methods for further details on polyclonal mouse anti-MPO IgG production.

Urine and plasma analysis of murine samples

Urine samples were collected from mice at varying time points using metabolic cages. Haematuria was assessed with dipstick (score 0-4) at day 1-7 using Combur-Test strips (Roche Diagnostics BV, Netherlands). Albuminuria (day 1 and 7) was measured by ELISA (quantitation kit; Bethyl Laboratories, USA) following the manufacturer's instructions. Plasma samples were tested for circulating anti-MPO antibody titres by ELISA at days 1 and 7 as described above using a serum pool from MPO immunized MPO-/- mice for reference as previously described[21].

Flow cytometry of murine samples

Automated total and differential white blood cell counts (WBC) were determined at time of sacrifice (day 1 and 7) using the Sysmex XT-1800iV (Sysmex, The Netherlands). Neutrophils ($Ly6G^{+}CD11b^{high}$) and monocytes ($Ly6G^{-}CD11b^{+}$) and their activation status, were analysed in peripheral blood by Flow cytometry on a Calibur flow cytometer (BD BioSciences). See supplemental materials and methods for further details.

Experimental autoimmune vasculitis protocol

EAV, a model of MPO-ANCA vasculitis, was induced in male and female rats, as previously described[19]. Unimmunised animals were included to provide a comparison to the basal state. Co-housed rats were randomly divided into 2 groups: vehicle or EDO-S101 (10 mg/kg) treated (n=7-8/group) and received treatment intravenously into the lateral tail vein starting at day 28 (baseline), given that we have previously shown well-established disease at day 28 in this model[20]. All rats were sacrificed at day 56. See supplemental materials and methods for further details.

The International Society of Nephrology (http://www.isn-online.org/site/cms)

For Peer Review Only

Urine and plasma analysis of rat samples

Urine samples were collected from rats at day 56 using metabolic cages and haematuria was assessed with dipstick (score 0-4) using Multistix (Siemens, Ireland). Albuminuria was measured by ELISA (Nephrat kit; Exocell, USA), following the manufacturer's instructions. Plasma samples were tested for circulating anti-human (h)MPO antibody titres by ELISA at day 56 as previously described[19,21]. See supplemental materials and methods for further details.

Flow cytometry of rat samples

Peripheral blood was taken from healthy controls, rats on day 28 post immunisation (baseline disease) and at the time of sacrifice (day 56) and analysed by flow cytometry to determine leukocyte subsets. Samples were analysed on a CyAn ADP analyser (Beckman Coulter). Subsequent analysis was performed using Kaluza v1.2 analysis software (Beckman Coulter). Frequencies and absolute numbers of the following leukocyte subsets were determined as: total leukocytes ($CD45^+$), neutrophils ($SSC^{hi}RP\text{-}1^+$), monocytes ($CD3^-CD4^+$), B cells ($CD45RA^+$), T cells ($CD3^+$), NK cells ($CD3^-CD161a^+$). See supplemental materials and methods for further details.

Cell viability and analysis of DNA content in human B cells

Seraphina BL cells were treated as described in figure legends with DMSO control, EDO-S101, Bendamustine (Sigma-Aldrich) or Vorinostat (Sigma-Aldrich). After the indicated times, cells were harvested and counted. Cell viability was analysed via an MTT assay. Additionally, PI-stained cells were analysed for DNA content by flow cytometry using a CyAn ADP analyser (Beckman Coulter). See supplemental materials and methods for further details.

Immunohistopathological Analysis

Activation of p53 induces the expression of a variety of gene products, which can in turn either prevent proliferation of damaged cells, or induce apoptosis, thereby removing damaged cells from

The International Society of Nephrology (http://www.isn-online.org/site/cms)

For Peer Review Only

the body[22]. Phosphorylation of H2AX plays a major role in the DNA damage response and is required for the assembly of DNA repair proteins[23]. Therefore, we investigated these molecules given their role in apoptosis and DNA damage[9,23]. For analysis of the xenograft model, selected tumours excised from treated and control mice were stained for anti-pH2AX and anti-p53 (Cell Signaling, Boston, MA). To further investigate the effect of EDO-S101 on DNA damage, rat spleen sections (10µm) were also stained for anti-pH2AX and anti-p53 (Cell Signaling, Boston, MA). For analysis of the vasculitis models, kidney sections (4µm) were stained with periodic acid-Schiff (PAS) and haematoxylin and eosin (H&E) to assess morphology as previously described[19-21,24]. In addition to kidney pathology, rats with EAV develop pulmonary vasculitis and haemorrhage as previously described[25]. See supplemental materials and methods for further details.

Statistical Analysis

All statistical analyses were performed using GraphPad Prism 6.0 software. Mouse haematuria and albuminuria were analysed using two-way ANOVA, including time as a variable. All other comparisons between two groups were evaluated using the nonparametric Mann-Whitney U test. Differences were considered statistically significant when $p < 0.05$. Data represent mean values per experimental group ±SEM.

For Peer Review Only

FIGURE LEGENDS

Figure 1: Induction of global Histone 3 hyperacetylation and increased DNA damage of tumor tissue following treatment with EDO-S101.

(A) Hyperacetylation of Histone 3 (H3) and specific lysine residues in HL60 cells following treatment with EDO-S101 compared with Bendamustine (Bend). **(B)** p53 and pH2AX staining on *in vivo* tumor tissue from Daudi Burkitt's lymphoma on samples taken at day 4 and 8, showing greater DNA repair response after a single dose of 40 mg/kg or 80 mg/kg EDO-S101, compared with vehicle. **Scale bars = 100 µm.**

Figure 2: Pre-treatment with EDO-S101 in mice modestly decreases albuminuria but has no effect on glomerular histopathology.

(A) Anti-MPO antibody titres after induction of anti-MPO IgG/LPS-mediated GN in mice at days 1 and 7. **(B)** Albuminuria was significantly reduced in EDO-S101 pre-treated mice, compared with vehicle controls. **(C)** Quantification of crescentic glomeruli showed no significant differences between treatment groups. **(D-K)** Representative glomerular histology in vehicle and EDO-S101 pre-treated mice. **(D+E)** Necrotic glomerulus (Periodic acid-Schiff stain) on day 1 after disease induction in vehicle and EDO-S101 pre-treated mice respectively. **(F+G)** Neutrophil staining (Ly6G) 1 day after disease induction from vehicle and EDO-S101 pre-treated mice respectively. **(H+I)** Overview of renal cortical tissue (H&E stain) on day 7 after disease induction with a similar number of glomerular crescents in both vehicle and EDO-S101 pre-treated mice (red arrows). **(J+K)** Crescentic glomeruli (H&E stain) in vehicle and EDO-S101 pre-treated mice respectively on day 7 after disease induction. Data represents mean ± SEM; *p<0.05. **Scale bars: D-G, J+K = 50 µm, H+I = 100 µm.**

Figure 3: EDO-S101 treatment in rats significantly decreases both haematuria and albuminuria and ameliorates proliferative and crescentic glomerulonephritis.

The International Society of Nephrology (http://www.isn-online.org/site/cms)

For Peer Review Only

(A) Anti-hMPO antibody titres at day 56 days after induction of EAV in rats. Treatment with EDO-S101 in EAV rats led to significantly reduced **(B)** haematuria **(C)** albuminuria and **(D)** Crescentic GN compared with vehicle treated controls at day 56. **(E-L)** Representative glomerular histology in vehicle and EDO-S101 treated rats. **(E)** Foci of interstitial infiltrates and red cell tubular casts (H&E stain; red arrows) in vehicle and **(F)** mild interstitial infiltrates in EDO-S101 treated rats. **(G)** Mild GN, intense peri-glomerular inflammation and red cell casts (H&E stain; red arrows) in vehicle-treated rats. **(H)** Focus on inflammatory tubular destruction in EDO-S101 treated rats (H&E). **(I+K)** Crescentic GN in vehicle treated rats with intense peri-glomerular inflammation and red cell casts (PAS stain; red arrows). **(J)** Mild GN in EDO-S101 treated rats with **(L)** focal glomerular necrosis and early crescent formation (PAS stain; red arrows). Data represents mean ± SEM; *p<0.05, **p<0.01. **Scale bars: E+F = 500 µm, G = 200 µm, H-J = 100 µm, K+L = 50 µm.**

Figure 4: Treatment with EDO-S101 significantly decreases lung haemorrhage in EAV rats.

(A+B) The macroscopic lung petechiae score was determined by assessment of the right lung of **(A)** vehicle and **(B)** EDO-S101 treated animals; lung haemorrhages highlighted by white arrows **(C+D)** Antemortem lung haemorrhage shown by the presence of Perl's positive cells (blue, red arrow) in the lungs of **(C)** vehicle and **(D)** EDO-S101 treated rats. Alveolar hypocellularity of **(E, G)** vehicle treated animals, with thickening of alveolar walls (arrow). EDO-S101 treated rats **(F, H)** had minimal alveolar wall thickening (H&E, 100 and 400X). **(I)** Lung petechiae score of vehicle and EDO-S101 treated rats. Data represents mean; *p<0.05. **Scale bars: C+D, G+H = 50 µm, E+F = 100 µm.**

Figure 5: Impact of treatment with EDO-S101 on relative myeloid cell fractions.

(A) Pre-treatment with EDO-S101 in mice significantly increased the percentage of monocytes from leukocytes at day 7. **(B)** In rats, treatment with EDO-S101 had no significant effect on the percentage of monocytes from leukocytes at day 56. **(C)** Pre-treatment with EDO-S101 in mice significantly increased the percentage of neutrophils from leukocytes at day 7. **(D)** In rats, treatment with EDO-

The International Society of Nephrology (http://www.isn-online.org/site/cms)

For Peer Review Only

S101 increased the percentage of neutrophils from leukocytes compared to vehicle controls. HC represents unimmunised healthy controls, while BL denotes baseline disease in rats (day 28 post-immunisation). Data represents mean ± SEM; ***p<0.001.

Figure 6: Treatment with EDO-S101 results in selective depletion of B cells and T cells in rats compared with vehicle treated controls.

(A) There was a non-significant trend towards a decrease in the percentage of NK cells from leukocytes compared with vehicle treated controls. There was a significant decrease in **(B)** B cell and **(C)** T cell percentages from leukocytes following treatment with EDO-S101 compared with vehicle treated controls. HC represents unimmunised healthy controls, while BL denotes baseline disease in rats (day 28 post-immunisation). Data represents mean ± SEM; **p<0.01, ***p<0.001.

Figure 7: Treatment with EDO-S101 induces apoptosis in a B cell line and increases DNA damage in EAV tissue.

(A) Seraphina BL cells were cultured at 1 x 10^6 cells/ml in the presence of increasing concentrations of EDO-S101, Bendamustine or Vorinostat, and viability of cells was assessed by MTT assay 16 hours later. Viability assessed at 6 hours is shown in Supplemental figure 9. **(B)** BL Cells were cultured in 25µM EDO-S101, Bendamustine or Vorinostat and cells were counted at indicated time points. **(C)** Percentage sub-diploid cells was measured from DNA content of treated cells. **(D)** BL cells were cultured in 25µM EDO-S101, Bendamustine or Vorinostat and harvested at the indicated time points then probed for levels of cleaved PARP (Asp 214). **(E-H)** Representative histograms of 16 hour treated cells, fixed and stained with PI for DNA content analysis. Representative photomicrographs of spleen tissue from **(I-K)** vehicle and **(L-N)** EDO-S101 treated rats stained for P53 and PH2AX are indicated. There is a clear induction of both markers in EDO-S101 treated rats, particularly **(M)** P53, which extends beyond the restricted white pulp staining observed in **(J)** vehicle treated animals. Error bars represent mean ± SEM; ***p<0.001. **Scale bars: I-N = 50 µm.**

The International Society of Nephrology (http://www.isn-online.org/site/cms)

For Peer Review Only

REFERENCES

1. Kallenberg CGM. Pathogenesis of ANCA-associated vasculitides. *Annals of the Rheumatic Diseases.* 2011;70(Suppl 1):i59-i63.
2. Jennette JC, Falk RJ. Pathogenesis of antineutrophil cytoplasmic autoantibody-mediated disease. *Nat Rev Rheumatol.* 2014;10(8):463-473.
3. Tesar V, Hruskova Z. Limitations of Standard Immunosuppressive Treatment in ANCA-Associated Vasculitis and Lupus Nephritis. *Nephron Clinical Practice.* 2014;128(3-4):205-215.
4. Frew AJ, Johnstone RW, Bolden JE. Enhancing the apoptotic and therapeutic effects of HDAC inhibitors. *Cancer Letters.* 2009;280(2):125-133.
5. Hancock WW, Akimova T, Beier UH, Liu Y, Wang L. HDAC inhibitor therapy in autoimmunity and transplantation. *Annals of the Rheumatic Diseases.* 2012;71(Suppl 2):i46-i54.
6. Mehrling T, Chen Y. The Alkylating-HDAC Inhibition Fusion Principle: Taking Chemotherapy to the Next Level with the First in Class Molecule EDO-S101. *Anti-Cancer Agents in Medicinal Chemistry.* 2016;16(1):20-28.
7. López-Iglesias AA, San-Segundo L, González-Méndez L, et al. The Alkylating Histone Deacetylase Inhibitor Fusion Molecule Edo-S101 Displays Full Bi-Functional Properties in Preclinical Models of Hematological Malignancies. *Blood.* 2014;124(21):2100-2100.
8. Kraus M, Bader J, Mehrling T, Driessen C. Edo- S101, a New Alkylating Histone-Deacetylase Inhibitor (HDACi) Fusion Molecule, Has Superior Activity Against Myeloma and B Cell Lymphoma and Strong Synergy with Proteasome Inhibitors in Vitro. *Blood.* 2014;124(21):2249-2249.
9. Di Benedetto A, Ercolani C, Mottolese M, et al. Analysis of the ATR-Chk1 and ATM-Chk2 pathways in male breast cancer revealed the prognostic significance of ATR expression. *Scientific Reports.* 2017;7(1):8078.
10. Drogaris P, Villeneuve V, Pomiès C, et al. Histone Deacetylase Inhibitors Globally Enhance H3/H4 Tail Acetylation Without Affecting H3 Lysine 56 Acetylation. *Scientific Reports.* 2012;2:220.
11. Wang Q, van Timmeren MM, Petersen AH, et al. Age-determined severity of anti-myeloperoxidase autoantibody-mediated glomerulonephritis in mice. *Nephrology Dialysis Transplantation.* 2017;32(2):254-264.
12. Copeland S, Warren HS, Lowry SF, et al. Acute Inflammatory Response to Endotoxin in Mice and Humans. *Clinical and Diagnostic Laboratory Immunology.* 2005;12(1):60-67.
13. Xiao H, Heeringa P, Liu Z, et al. The Role of Neutrophils in the Induction of Glomerulonephritis by Anti-Myeloperoxidase Antibodies. *The American Journal of Pathology.* 2005;167(1):39-45.
14. Ciavatta DJ, Yang J, Preston GA, et al. Epigenetic basis for aberrant upregulation of autoantigen genes in humans with ANCA vasculitis. *J Clin Invest.* 2010;120(9):3209-3219.
15. McInnis EA, Badhwar AK, Muthigi A, et al. Dysregulation of autoantigen genes in ANCA-associated vasculitis involves alternative transcripts and new protein synthesis. *J Am Soc Nephrol.* 2015;26(2):390-399.
16. Besse L, Kraus M, Besse A, Bader J, Mehrling T, Driessen C. The First in Class, Alkylator-Histone-Deacetylase-Inhibitor Fusion Molecule Edo-S101 in Combination with Proteasome Inhibitors Induces Highly Synergistic Pro-Apoptotic Signaling through UPR Activation and Suppression of c-Myc and BCL2 in Multiple Myeloma. *Blood.* 2016;128(22):4466-4466.
17. De Filippi R, Crisci S, Cillo M, et al. The First-in-Class Alkylating Histone-Deacetylase Inhibitor (HDACi) Fusion Molecule Edo-S101 Exerts Potent Preclinical Activity Against Tumor Cells of Hodgkin Lymphoma (HL) Including Bendamustine-Resistant Clones. *Blood.* 2015;126(23):2481-2481.

For Peer Review Only

18. López-Iglesias AA, Herrero AB, San-Segundo L, et al. The Hybrid Molecule, Edo-S101, Impairs Double Strand Breaks Repair in Multiple Myeloma and Synergizes with Bortezomib and Dexamethasone. *Blood.* 2015;126(23):5354-5354.
19. Little MA, Smyth L, Salama AD, et al. Experimental Autoimmune Vasculitis : An Animal Model of Anti-neutrophil Cytoplasmic Autoantibody-Associated Systemic Vasculitis. *The American Journal of Pathology.* 2009;174(4):1212-1220.
20. O'Reilly VP, Wong L, Kennedy C, et al. Urinary Soluble CD163 in Active Renal Vasculitis. *Journal of the American Society of Nephrology.* 2016.
21. Little MA, Bhangal G, Smyth CL, et al. Therapeutic Effect of Anti–TNF-α Antibodies in an Experimental Model of Anti-Neutrophil Cytoplasm Antibody–Associated Systemic Vasculitis. *Journal of the American Society of Nephrology.* 2006;17(1):160-169.
22. Caspari T. Checkpoints: How to activate p53. *Current Biology.* 2000;10(8):R315-R317.
23. Podhorecka M, Skladanowski A, Bozko P. H2AX Phosphorylation: Its Role in DNA Damage Response and Cancer Therapy. *Journal of Nucleic Acids.* 2010;2010:9.
24. Xiao H, Heeringa P, Hu P, et al. Antineutrophil cytoplasmic autoantibodies specific for myeloperoxidase cause glomerulonephritis and vasculitis in mice. *The Journal of Clinical Investigation.* 2002;110(7):955-963.
25. Al-Ani B, Fitzpatrick M, Al-Nuaimi H, et al. Changes in urinary metabolomic profile during relapsing renal vasculitis. *Scientific Reports.* 2016;6:38074.

For Peer Review Only

AUTHOR CONTRIBUTIONS

DD participated in collection and/or assembly of data, data analysis/interpretation, and manuscript writing. MMvT, VOR and EOB participated in the study design and data analysis/interpretation. GB, BF, FH, EL, CP and FT participated in the data analysis/interpretation and manuscript writing. TH, PH and ML participated in the study design, conception and coordination and helped to draft the final manuscript. All authors read and approved the final manuscript.

ACKNOWLEDGEMENTS

This study was supported by Science Foundation Ireland grant 11/Y/B2093. FWKT is supported by the Diamond Fund from Imperial College Healthcare Charity and Ken and Mary Minton Chair of Renal Medicine.

DISCLOSURE

TM is an employee of Mundipharma-EDO GmbH. FWKT has received research project grants from AstraZeneca Limited, Baxter Biosciences, Boehringer Ingelheim, and MedImmune, and has consultancy agreements with Rigel Pharmaceuticals, Novartis and Baxter Biosciences. CDP has received a research project grant from GlaxoSmithKline. The experimental work was funded by Mundipharma.

For Peer Review Only

Figure 1

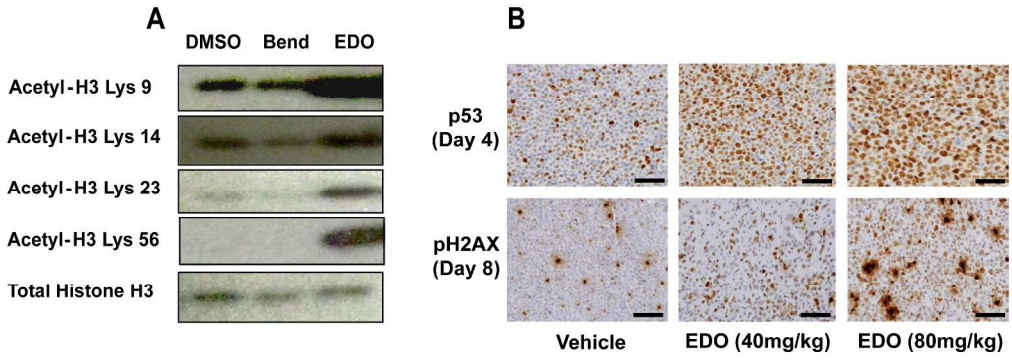

Figure 1: Induction of global Histone 3 hyperacetylation and increased DNA damage of tumor tissue following treatment with EDO-S101.

248x116mm (300 x 300 DPI)

For Review Only

Figure 2

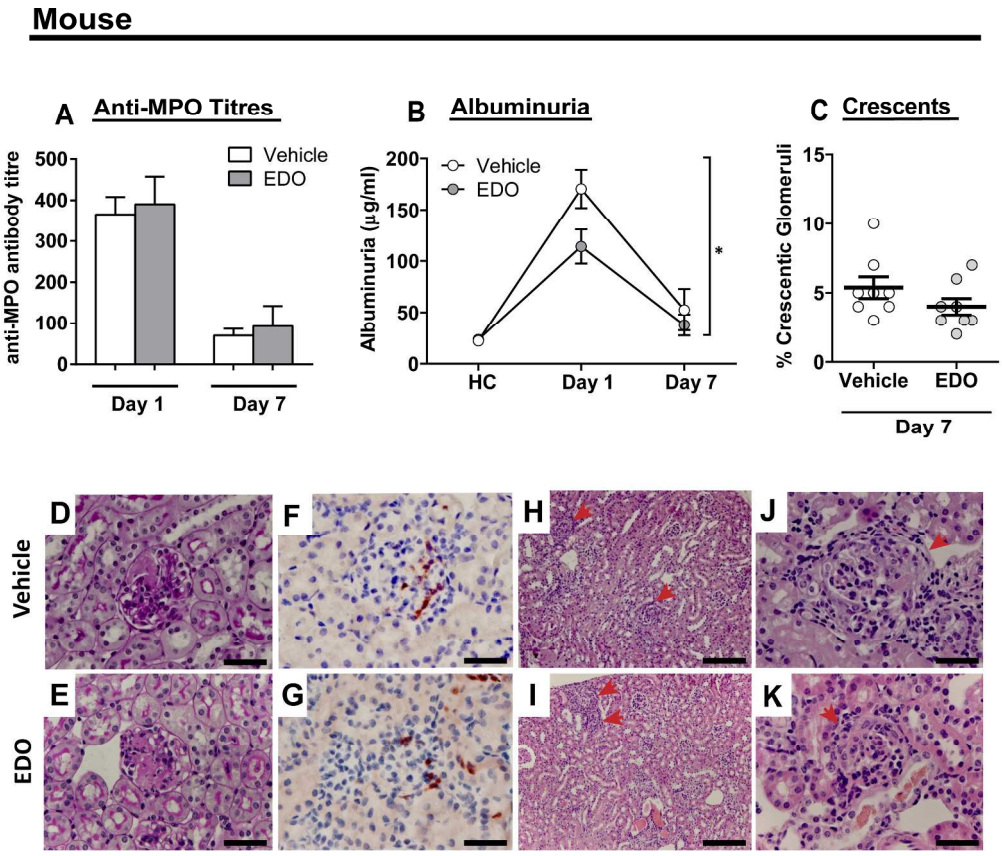

Figure 2: Pre-treatment with EDO-S101 in mice modestly decreases albuminuria but has no effect on glomerular histopathology.

247x233mm (300 x 300 DPI)

Figure 3

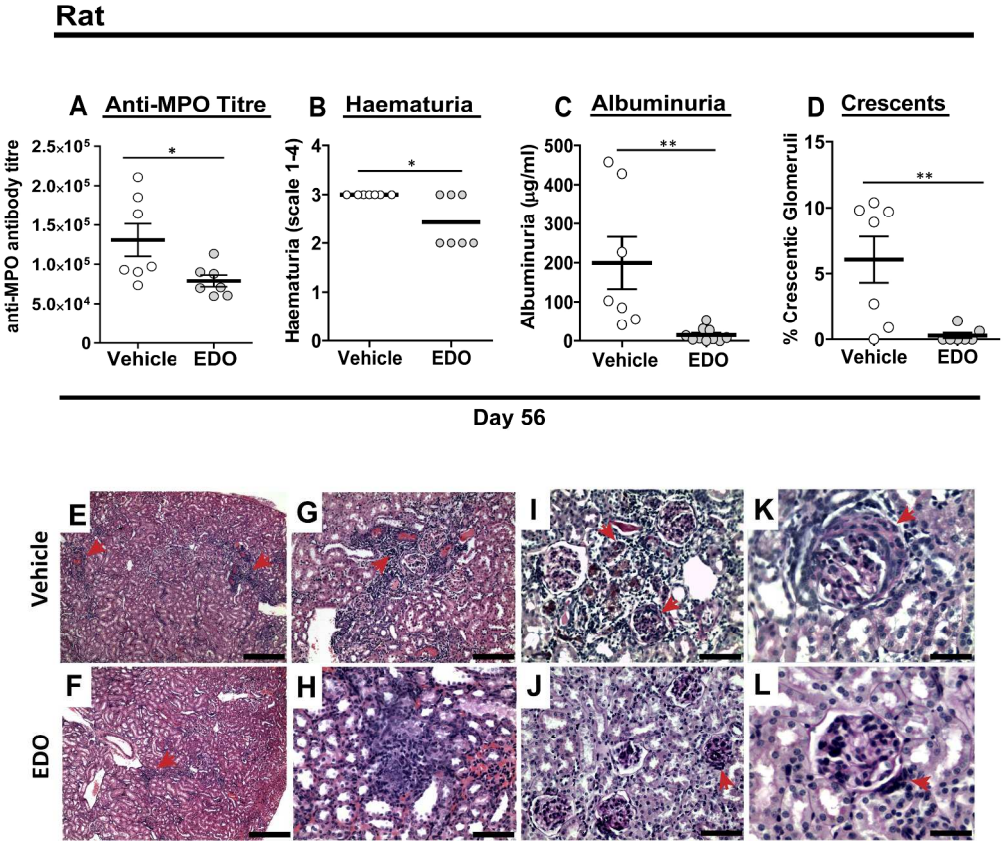

Figure 3: EDO-S101 treatment in rats significantly decreases both haematuria and albuminuria and ameliorates proliferative and crescentic glomerulonephritis.

255x239mm (300 x 300 DPI)

Figure 4

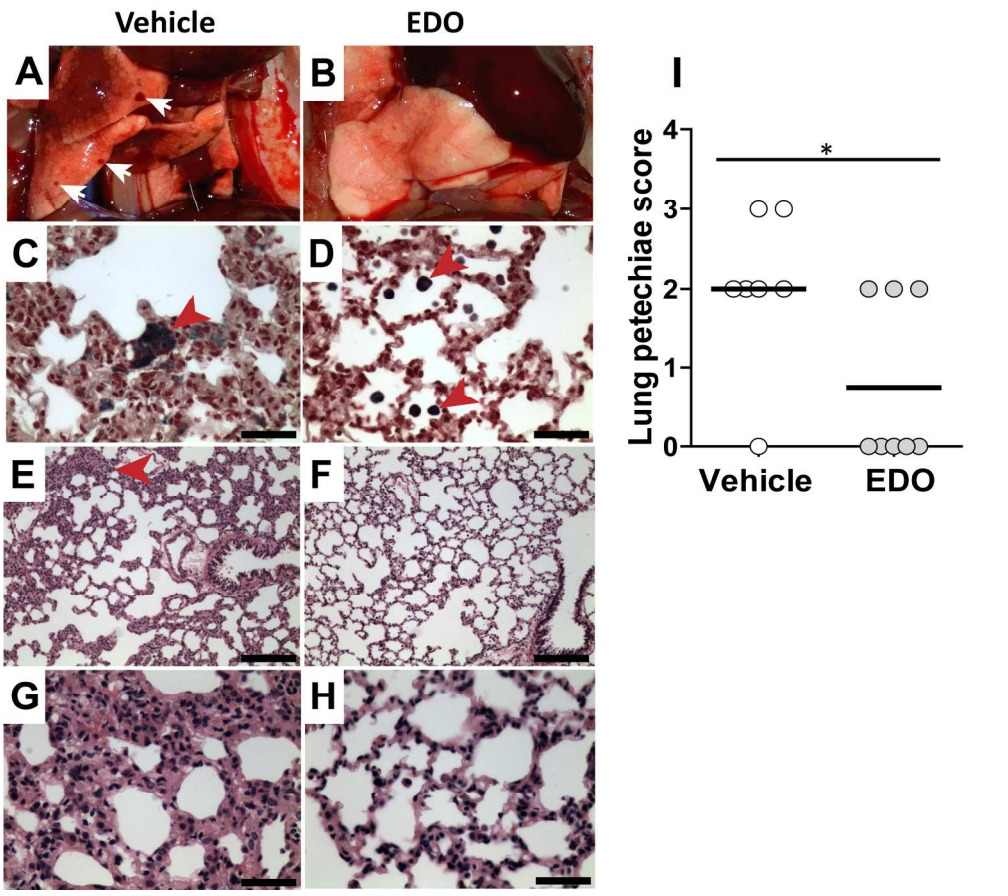

Figure 4: Treatment with EDO-S101 significantly decreases lung haemorrhage in EAV rats.

199x215mm (300 x 300 DPI)

Figure 5

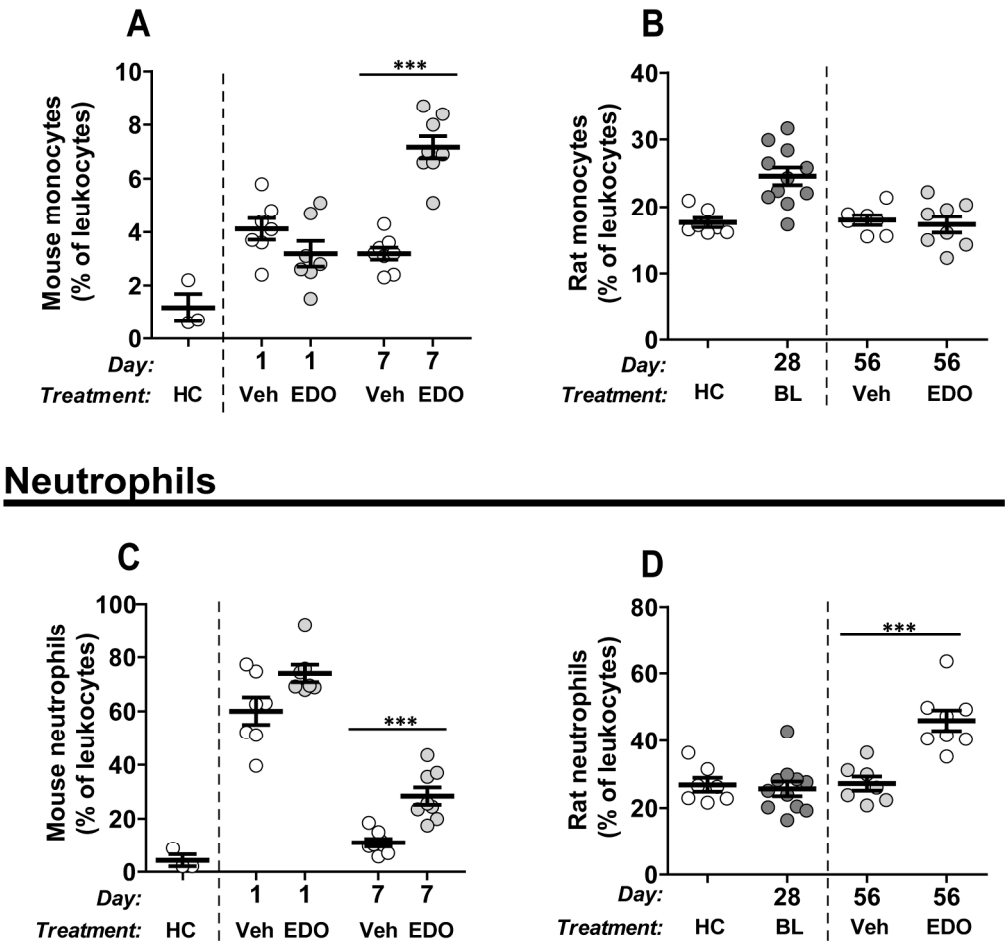

Figure 5: Impact of treatment with EDO-S101 on relative myeloid cell fractions.

204x234mm (300 x 300 DPI)

Figure 6

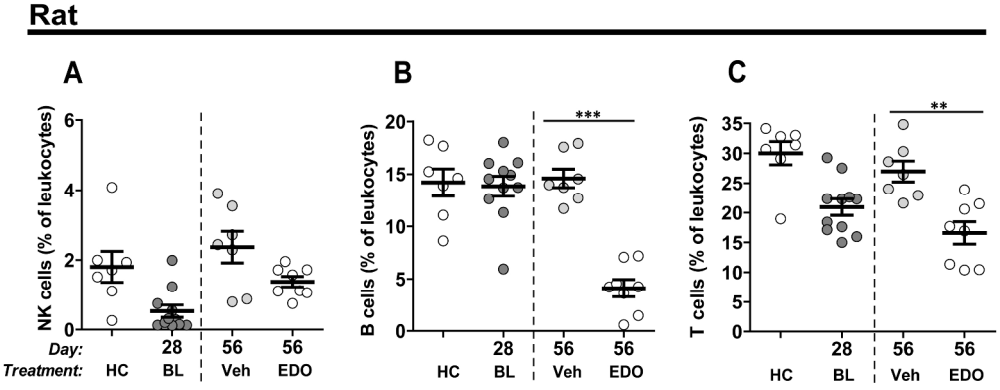

Figure 6: Treatment with EDO-S101 results in selective depletion of B cells and T cells in rats compared with vehicle treated controls.

258x124mm (300 x 300 DPI)

For Review Only

Figure 7

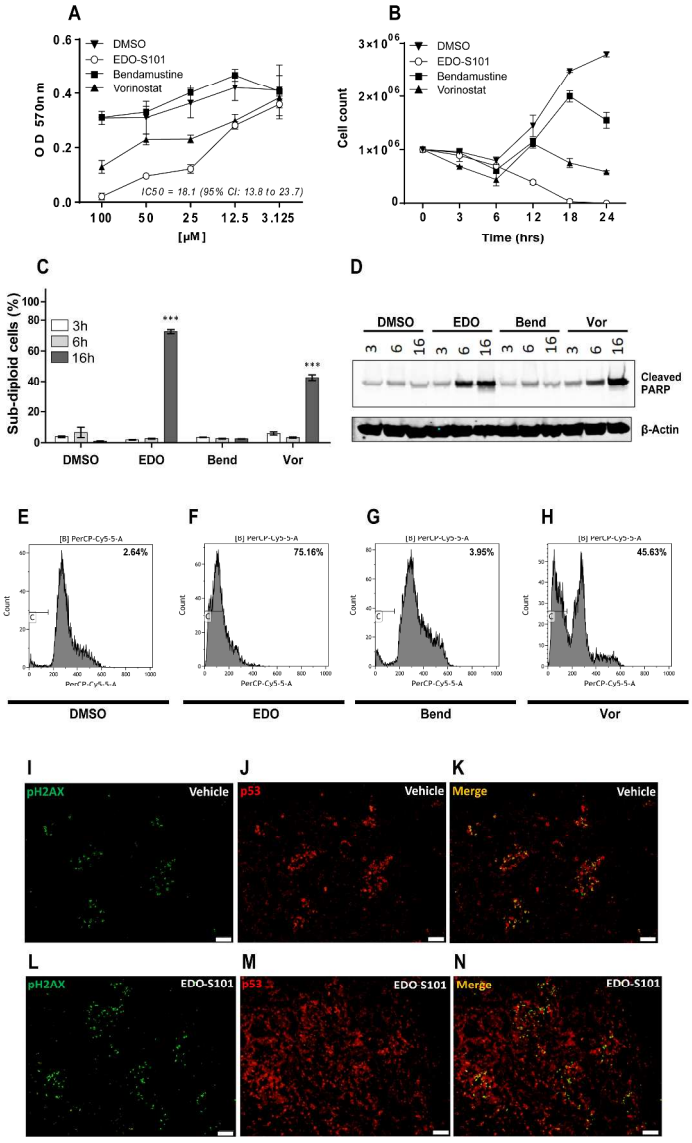

Figure 7: Treatment with EDO-S101 induces apoptosis in a B cell line and increases DNA damage in EAV tissue.

261x441mm (300 x 300 DPI)

Supplemental Figure 1

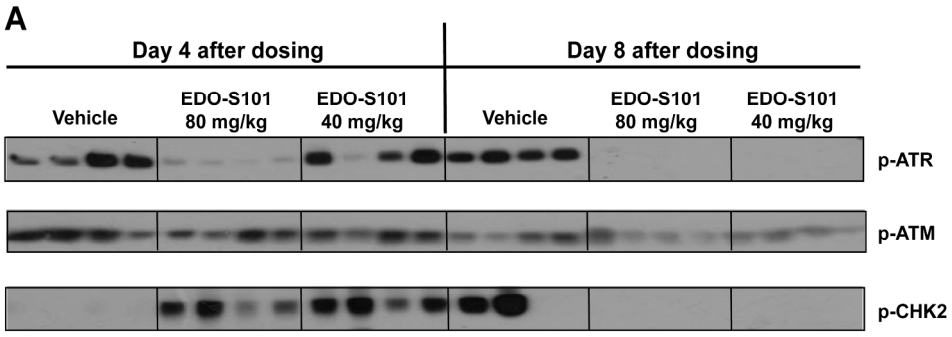

229x115mm (300 x 300 DPI)

For Review Only

Supplemental Figure 2

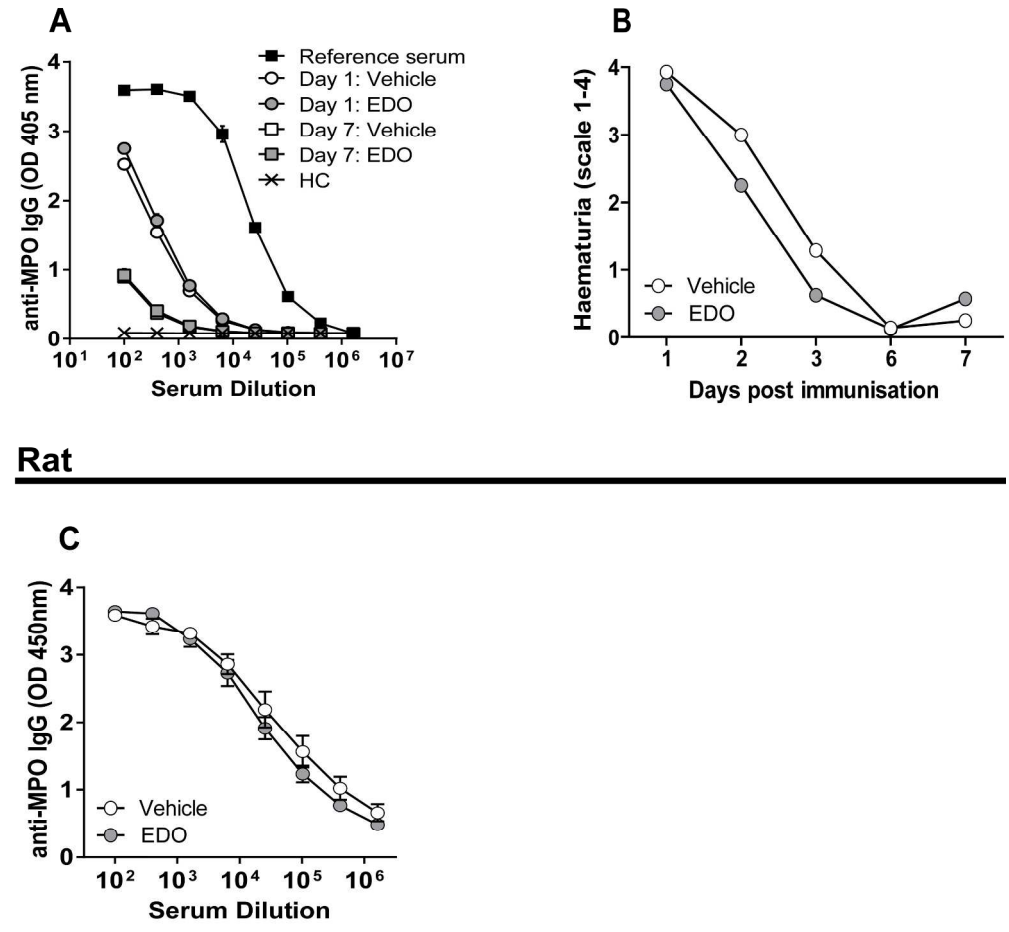

225x245mm (300 x 300 DPI)

Supplemental Figure 3

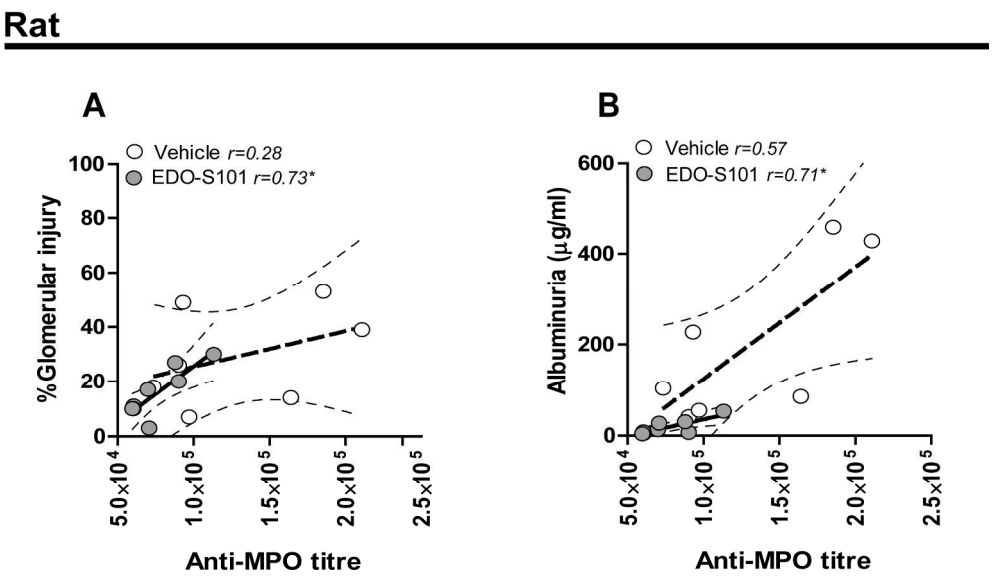

221x151mm (300 x 300 DPI)

For Peer Review Only

Supplemental Figure 4

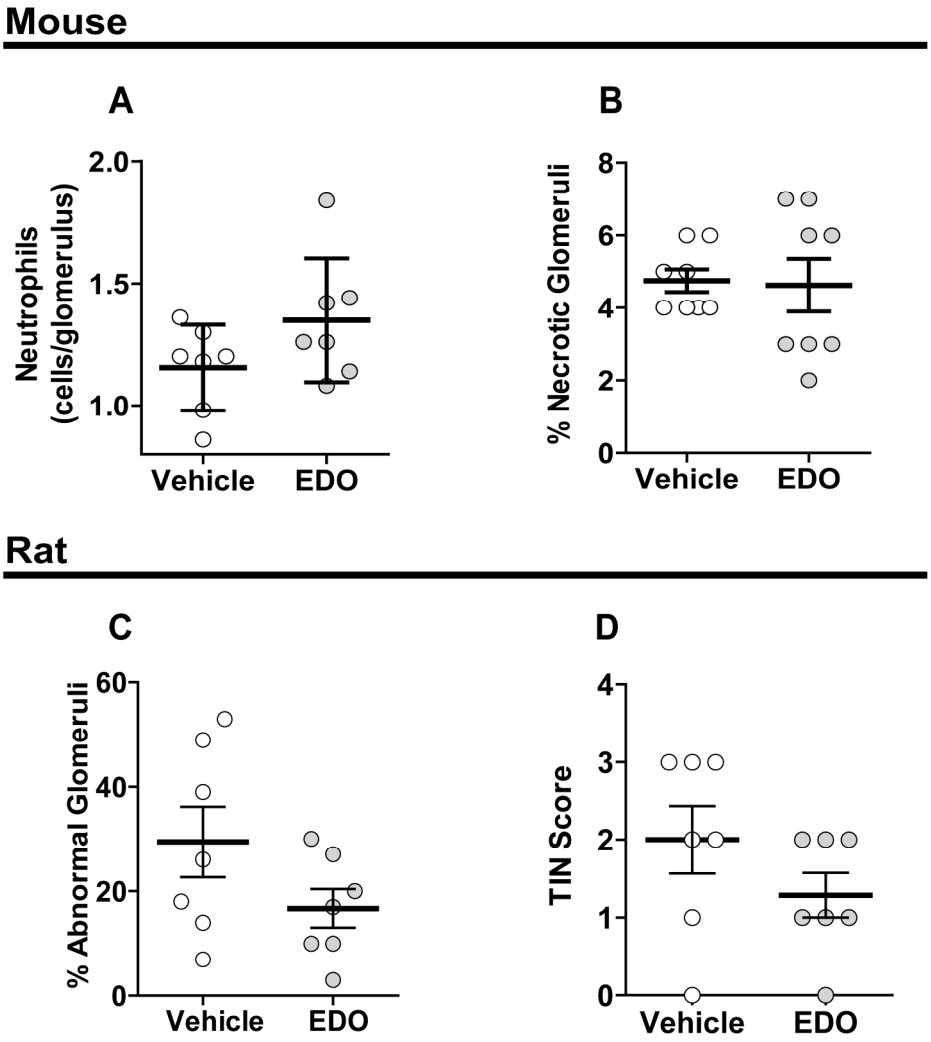

196x241mm (300 x 300 DPI)

Supplemental Figure 5

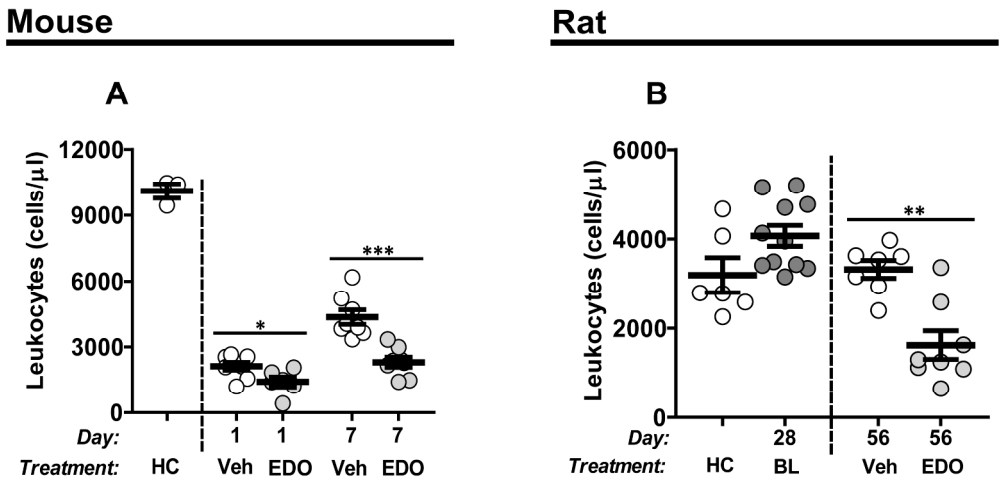

231x138mm (300 x 300 DPI)

For Review Only

Supplemental Figure 6

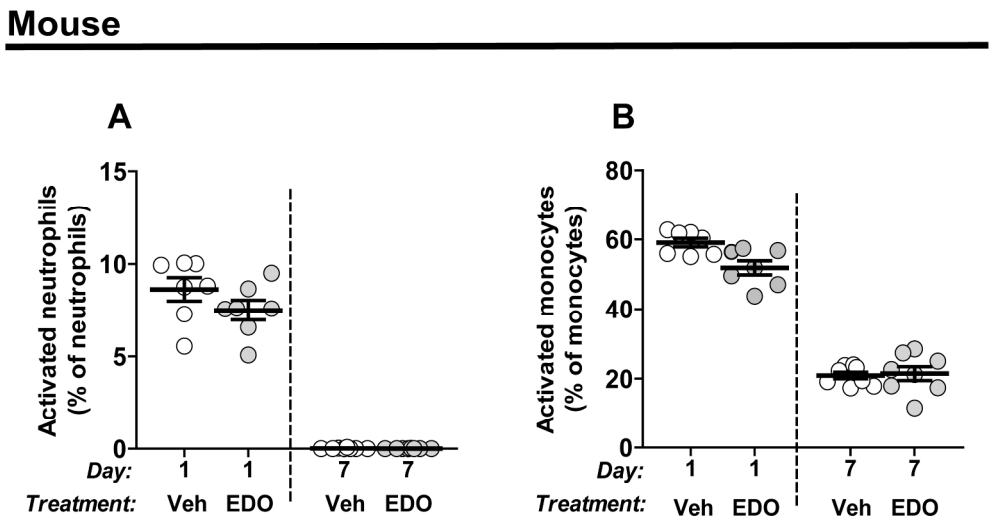

217x137mm (300 x 300 DPI)

For Peer Review Only

Supplemental Figure 7

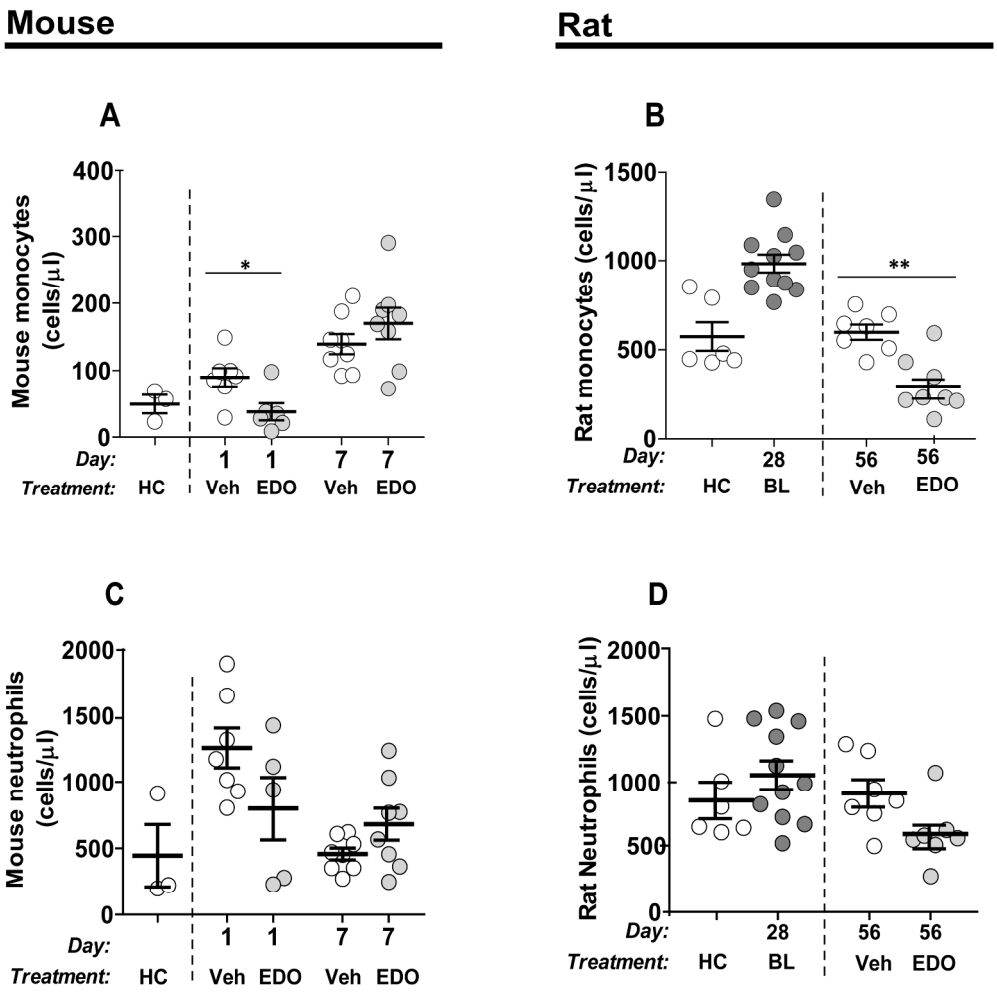

227x252mm (300 x 300 DPI)

Supplemental Figure 8

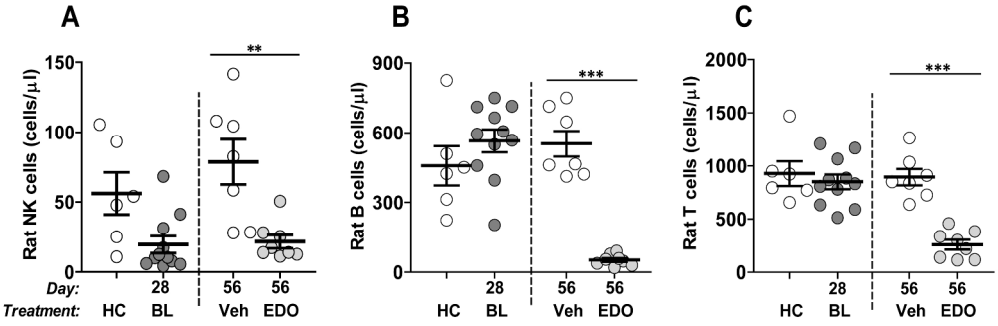

257x125mm (300 x 300 DPI)

For Review Only

Supplemental Figure 9

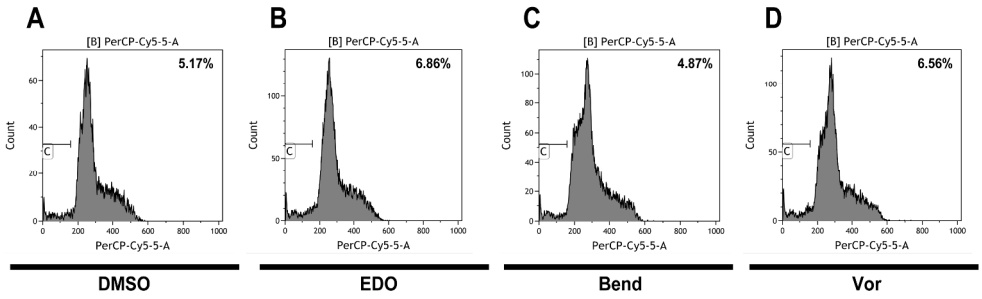

259x113mm (300 x 300 DPI)

For Peer Review Only

SUPPLEMENTARY FIGURE LEGENDS

Supplementary Figure 1: DNA repair response in tumor samples following treatment with EDO-S101.

(A) DNA repair response taken from Daudi Burkitt's lymphoma samples at day 4 and 8 after dosing. P-ATR and p-ATM are dose dependently suppressed by EDO-S101, while p-CHK2 is strongly elevated at day 4 but returns to undetectable leves at day 8.

Supplementary Figure 2: Pre-treatment with EDO-S101 in mice has no effect on haematuria.

(A) Urinalysis and anti-MPO antibody titration curves after induction of anti-MPO IgG/LPS-mediated GN in mice days 1 and 7. **(B)** Haematuria score in vehicle and EDO-S101 pre-treated mice was highest at day 1 and gradually decreased in time, with no significant effect of EDO-S101 pre-treatment. **(C)** Anti-hMPO antibody titration curves 56 days after induction of EAV in rats at day 56. Data represents mean ± SEM.

Supplementary Figure 3: Pre-treatment with EDO-S101 in mice has no effect on glomerular histopathology and EDO-S101 treatment in rats has no effect on proliferative GN or TIN score.

(A) Quantification of glomerular neutrophils (Ly6G) 1 day after disease induction in mice showed no significant differences between treatment groups. **(B)** Quantification of necrotic or abnormal glomeruli (Periodic acid-Schiff stain) 1 day after disease induction in mice showed no significant differences between treatment groups. **(C)** Quantification of proliferative GN (proportion of glomeruli classified as abnormal) was non-significantly decreased in EDO-S101 treated rats compared with vehicle treated controls. **(D)** There was no significant difference in tubulointerstitial nephritis (TIN) score in EDO-S101 treated compared with vehicle treated rats. Data represents mean ± SEM.

For Peer Review Only

Supplementary Figure 4: EDO-S101 induces a significant correlation between anti-MPO titre and urine/histology abnormalities in the rat model.

Correlation analysis showed a significant correlation between anti-MPO titre and **(A)** glomerular injury and **(B)** albuminuria (r>0.7) in the EDO-S101 treated group.

Supplementary Figure 5: Pre-treatment and treatment with EDO-S101 induced leukopenia in both mouse and rat models.

(A) At days 1 and 7, total leukocyte counts were significantly lower in mice which received EDO-S101 compared with vehicle controls. **(B)** At day 56, treatment with EDO-S101 significantly reduced leukocyte counts in rats compared with vehicle treated controls, suggesting that EDO-S101 induces leukopenia in both models. The normal leukocyte range is indicated in healthy controls (HC) in both mice and rats. Baseline (BL) in rats denotes baseline disease, before treatment with EDO-S101 (day 28 post-immunisation). Data represents mean ± SEM; *p<0.05, **p<0.01, ***p<0.001.

Supplementary Figure 6: Impact of treatment with EDO-S101 on mouse myeloid cell activation.

There was no significant effect of EDO-S101 pre-treatment on the percentage of activated **(A)** neutrophils or **(B)** monocytes compared with vehicle controls on day 1 or day 7. Data represents mean ± SEM.

Supplementary Figure 7: Treatment with EDO-S101 decreases the number of circulating monocytes in both mice and rats.

(A) At day 1, pre-treatment with EDO-S101 in mice significantly reduced the circulating monocyte count compared with vehicle controls. **(B)** In rats, treatment with EDO-S101 significantly reduced the circulating monocyte count compared with vehicle controls at day 56. There was no significant effect of EDO-S101 treatment on circulating neutrophil counts in **(C)** mice or **(D)** rats. HC represents

For Peer Review Only

unimmunised healthy controls, while BL denotes baseline disease in rats (day 28 post-immunisation). Data represents mean ± SEM; *p<0.05, **p<0.01, ***p<0.001.

Supplementary Figure 8: Treatment with EDO-S101 results in selective depletion of NK cells, B cells and T cells in rats compared with vehicle treated controls.

(A) Circulating NK cells were elevated in rats which received vehicle compared with baseline levels, however, treatment with EDO-S101 blocked this increase and resulted in a significant decrease in NK cells. There was also a significant decrease in **(B)** B cells and **(C)** T cells following treatment with EDO-S101 compared with vehicle treated controls. HC represents unimmunised healthy controls, while BL denotes baseline disease in rats (day 28 post-immunisation). Data represents mean ± SEM; **p<0.01, ***p<0.001.

Supplementary Figure 9: DNA content analysis in B cells following 6-hour treatment with EDO-S101.

(A-D) BL cells were cultured in 25μM EDO-S101, Bendamustine (Bend) or Vorinostat (Vor) for 6 hours, then fixed and stained with PI for DNA content analysis.

For Peer Review Only

SUPPLEMENTAL MATERIALS AND METHODS

Animals

Female Mus musculus NOD/SCID female mice from HFK Bio-Technology Co. Ltd. (Beijing, China) were used for the xenograft model. $MPO^{-/-}$ mice (B6.129X1-MPO^{tm1Lus}/J) were purchased from Jackson Laboratories (Bar Harbor, Maine) and bred in-house. Female C57BL/6J mice (8-10 weeks old) were purchased from Harlan (Horst, The Netherlands). Wistar–Kyoto (WKY) rats were derived from the inbred colony of authors CDP and FT and bred by Charles River (Margate, UK). Equal numbers of male and female rats (6-weeks old) were used throughout the experiment in both treatment groups. All animals were housed with access to food and water ad libitum in a 22° temperature-controlled facility with a 12-hour light/dark cycle. All experiments were approved by the local ethical committees and performed according to the guidelines described on the protection of animals used for scientific purposes at University Medical Centre Groningen, Trinity College Dublin and Mundipharma-EDO GmbH (EU Directive 2010/63).

Mouse Xenograft Model

A mouse xenograft model was used for investigating the DNA damaging effects of EDO-S101 in tumour tissue as previously described[1]. Briefly, each mouse was inoculated subcutaneously in the right flank region with Daudi tumour cells (1×10^7) in 0.1ml of PBS/Matrigel (1:1). Mice were randomised to treatment with vehicle or EDO-S101 (40 and 80mg/kg) and sacrificed 4 or 8 days later. The compound was prepared and administered intravenously into a lateral tail vein as described previously[1]. Briefly, EDO-S101 stock (50 mM in DMSO) was combined at a final concentration of 6mg/mL with a 1:1:1 mixture of 50% (v/v) acetic acid, 30% (w/w) Hydroxypropyl beta-Cyclodextrin (HPBCD) and 2.5% $NaHCO_3$.

Western Blotting

For Peer Review Only

Cells were centrifuged at 10,000 g for 2 min, washed with PBS and lysed in ice-cold lysis buffer (140 mM NaCl, 10 mM EDTA, 10% glycerol, 1% Nonidet P-40, 20 mM Tris (pH 7.0), 1 µM pepstatin, 1 µg/ml aprotinin, 1 µg/ml leupeptin, 1 mM sodium orthovanadate). Western blots were probed with antibodies to p-ATR, p-ATM, Chk2, cleaved PARP Asp214 (Cell Signalling, Boston, MA) and β-Actin (Sigma-Aldrich).

Polyclonal Mouse Anti-MPO IgG Production

$MPO^{-/-}$ mice received 10 µg of murine MPO intraperitoneally (i.p.) in complete Freund's adjuvant (CFA) (Difco, Detroit, MI) on day 0, followed by i.p. booster injections in incomplete Freund's adjuvant (Difco, Detroit, MI) on days 21 and 36, with exsanguination on day 42. Antibody titres were monitored by ELISA. In short, microtitre plates were coated overnight with murine MPO (0.5 µg/ml) and blocked with BSA. Plates were then incubated with mouse sera (1:100 starting dilution), followed by incubation with alkaline phosphatase-conjugated goat anti-mouse IgG antibodies (A4656, Sigma-Aldrich). 4-Nitrophenyl phosphate (pNPP; P5994, Sigma-Aldrich) was used as substrate and wells were analysed spectrophotometrically at 405 nm. IgG was isolated from pooled sera using a HiTrap Protein GHP column (GE Healthcare Europe GmbH, Netherlands). IgG containing fractions were pooled and dialysed against PBS. Protein concentrations were determined using the bicinchoninic acid protein assay kit (Thermo Fisher Scientific, Rockford, IL). The anti-MPO titre of the new batch was confirmed by ELISA as described above, using a sample of anti-MPO IgG with previously established pathogenicity as a reference.

Murine passive transfer vasculitis disease induction and treatment protocol

Male and female C57Bl/6J mice were randomly divided into 4 groups: vehicle pre-treated and sacrificed at day 1 or 7 (n=8/group) or EDO-S101 pre-treated and sacrificed at day 1 or 7 (n=8/group). Mice received EDO-S101 (25 mg/kg) or vehicle intravenously (i.v) one day before disease induction. On the next day, disease was induced via i.v. administration of 1.5 mg of anti-

For Peer Review Only

MPO IgG, followed by LPS administration i.p. (5 µg/g) 1 hour later (Escherichia coli, serotype O26:B6; Sigma -Aldrich).

Flow cytometry of murine samples

Automated total and differential white blood cell counts (WBC) were determined at time of sacrifice (day 1 and 7) using the Sysmex XT-1800iV (Sysmex, The Netherlands). Neutrophils ($Ly6G^+CD11b^{high}$) and monocytes ($Ly6G^-CD11b^+$) and their activation status, were analysed in peripheral blood by Flow cytometry. In short, 100 µl of whole blood was stained with an antibody cocktail consisting of: rat anti-mouse CD11b-PE (Clone: M1/70, BD BioSciences), hamster anti-mouse CD80-APC (Clone: 16-10A1, BD BioSciences), rat anti-mouse Ly6G-FITC (Clone: 1A8, BD BioSciences) and rat anti-mouse CD62L-PerCP-Cy5.5 (Clone: MEL-14, BD BioSciences) for 30 minutes at 4°C in the dark. Red blood cells were lysed using BD FACS lysing solution diluted 1:10 in dH2O. After washing with PBS supplemented with 5% FCS, cells were resuspended in PBS+5% FCS and analysed on a Calibur flow cytometer (BD BioSciences). Subsequent analyses were done with Kaluza v1.2 analysis software (Beckman Coulter). For neutrophil sorting, granulocytes were gated based on forward scatter (FSC) and side scatter (SSC). Neutrophils were then identified as Ly6G-positive and CD11b-high positive ($Ly6G^+CD11b^{high}$). Activated neutrophils were identified as those negative for CD62L ($Ly6G^+CD11b^{high}CD62L^-$). For monocyte sorting, cells were first gated based on FSC and SSC and then identified as Ly6G-negative, CD11b-positive cells ($Ly6G^-CD11b^+$). Activated monocytes were identified as CD80-positive ($Ly6G^-CD11b^+CD80^+$).

Experimental autoimmune vasculitis protocol

EAV, a model of MPO-ANCA vasculitis, was induced in in male and female rats, as previously described[2]. Briefly, 6-week-old WKY rats were immunised with 3.2 mg/kg human MPO administered intramuscularly and subcutaneously in CFA (Merck 475911, Nottingham, UK), along with 1 µg of Pertussis toxin i.p. (Sigma-Aldrich, St. Louis, MO). Rats were boosted with 4 mg LPS and 0.1 mg/kg

For Peer Review Only

MPO (without adjuvant) i.p. after 28 and 35 days, respectively. Unimmunised animals were included to provide a comparison to the basal state. Co-housed rats were randomly divided into 2 groups: vehicle or EDO-S101 (prepared as described above) treated (n=7-8/group) and received treatment intravenously into the lateral tail vein starting at day 28 (baseline), given that we have previously shown well-established disease at day 28 in this model[3]. Preliminary work showed excessive weight loss with 25 mg/kg EDO-S101 (data not shown), so rats were treated with a dose of 10 mg/kg weekly, which was well tolerated throughout the study. All rats were sacrificed at day 56.

Urine and plasma analysis of rat samples

Urine samples were collected from rats at day 56 using metabolic cages and haematuria was assessed with dipstick (score 0-4) using Multistix (Siemens, Ireland). Albuminuria was measured by ELISA (Nephrat kit; Exocell, USA), following the manufacturer's instructions. Plasma samples were tested for circulating anti-human (h)MPO antibody titres by ELISA at day 56 as previously described[2,4]. Briefly, 96-well plates were coated overnight with hMPO (2 µg/ml) in carbonate buffer. Wells were incubated with dilutions of serum samples in triplicate for 1 hour at RT, washed, and incubated with anti-rat IgG-alkaline phosphatase conjugate (Sigma, USA) for 1 hour at RT. Binding was detected with p-NPP (Sigma) and read at 405 nm.

Flow cytometry of rat samples

Peripheral blood was taken from healthy controls, rats on day 28 post immunisation (baseline disease) and at the time of sacrifice (day 56) and analysed by flow cytometry to determine leukocyte subsets. Frequencies and absolute numbers of the following leukocyte subsets were determined as: total leukocytes ($CD45^+$), neutrophils ($SSC^{hi}RP\text{-}1^+$), monocytes ($CD3^-CD4^+$), B cells ($CD45RA^+$), T cells ($CD3^+$), NK cells ($CD3^-CD161a^+$). Samples were stained for 20 minutes in the dark with anti-CD45 PE-Cy7 (Clone: OX-1, BD Biosciences), anti-RP-1 PE (rat neutrophils, clone: RP-1, BD Biosciences), anti-CD4 APC (Clone: OX-35, BD Biosciences), anti-CD45RA PE-Cy5 (rat B-cells, Clone: OX-33, BD

For Peer Review Only

Biosciences), anti-CD3 V421 (Clone: 1F4, BD Biosciences), anti-CD161a FITC (rat NK cells, Clone: 10/78, BD Biosciences). Red blood cells were lysed with BD FACS lysing solution as above. After washing with PBS supplemented with 5% FCS, cells were resuspended in PBS+5% FCS and analysed on a CyAn ADP analyser (Beckman Coulter). Single stain One Comp beads (eBioscience) and fluorescence minus one (FMO) controls were used to correct for spectral overlap and non-specific staining respectively. Subsequent analysis was performed using Kaluza v1.2 analysis software (Beckman Coulter).

Cell viability analysis by cell counting and MTT assay in human B cells

Seraphina Burkitt Lymphoma cells were seeded into 96 well plates and treated as described in figure legends with DMSO control, EDO-S101, Bendamustine (Sigma-Aldrich) or Vorinostat (Sigma-Aldrich). After the indicated times, cells were harvested and counted. Seraphina Burkitt Lymphoma cells were seeded into 96 well plates and treated as described in figure legends. Media was removed and the cells were washed once with PBS. 200µl per well of 1mg/ml MTT solution (Thiazolyl Blue Tetrazolium Bromide) (Sigma-Aldrich) was added directly to the cells and the plates were incubated at 37°C for 2h in the dark. After incubation, MTT solution was discarded and 200µl per well of DMSO solution was added for 20min at 37°C in the dark. Absorbance was read at λ=570nm.

Analysis of DNA content by PI staining in human B cells

Cells were harvested and fixed in 70% ethanol in PBS overnight at 4°C. Fixed cells were washed three times in 1 ml cold PBS, resuspended in 500 µl 50-µg/ml propidium iodide (PI) (Sigma-Aldrich) in PBS containing RNase-A (0.5 mg/ml), and incubated for 30 min at 37°C prior to analysis. PI-stained cells were then analysed for DNA content by flow cytometry. Samples were analysed on a CyAn ADP analyser (Beckman Coulter). Subsequent analysis was performed using Kaluza v1.2 analysis software (Beckman Coulter).

For Peer Review Only

Immunohistopathological Analysis

For analysis of the xenograft model, immunohistochemical studies were performed on selected tumours excised from treated and control mice. After fixation for 24h in paraformaldehyde 10%, 3µm sections were prepared with a manual tissue arrayer (Beecher Instruments, Sun Prairie, WI, USA). Incubation with primary and secondary antibodies was performed with a semi-automatic Dako Autostainer (DAKO, Carpinteria, CA, USA) system. Primary antibodies included anti-pH2AX and anti-p53 (Cell Signaling, Boston, MA). HRP-conjugated secondary antibody was from Envision system (DAKO ref K5007). Staining was performed with the IHC DAB MAP system (Ventana Medical Systems, Tucson, AR, USA). Sections were then counterstained with haematoxylin and eosin (H&E).

For analysis of the vasculitis models, kidney tissues were harvested, fixed in 10% buffered formalin, embedded in paraffin wax, and sectioned at 4µm thickness. Sections were stained with periodic acid-Schiff (PAS), H&E to assess morphology and to establish the incidence of fibrinoid necrosis and crescent formation respectively, as previously described[2-5]. Glomerular neutrophils were identified by staining with LY6G. In addition to kidney pathology, rats with EAV develop pulmonary vasculitis and haemorrhage. This was assessed macroscopically by a visual inspection of the lungs at the time of killing and graded according to the amount of lung surface bleeding (lung petechiae score) as follows: 0 = no haemorrhage; 1 = 1 haemorrhage; 2 = 2-5 haemorrhages; 3 = 6-12 haemorrhages and 4 = >12 haemorrhages. Rat lung tissue was subsequently harvested and stained with H&E. Hemosiderin-laden macrophages (and hence ante-mortem lung haemorrhage) were identified using Perl's Prussian blue stain as previously described[6]. To investigate the effect of EDO-S101 on DNA damage in rat, spleen tissue was harvested, fixed in Periodate-Lysine-Paraformaldehyde, and cryosectioned at a thickness of 10µm. Sections were incubated with primary antibodies; anti-pH2AX and anti-p53 (1:100 and 1:600 respectively; Cell Signaling, Boston, MA) for 2hr at RT followed by 1 hr secondary antibody incubation: Alexa Fluor® 488 and 568 (1:250; ThermoFisher Scientific). Hoechst (1:1000; Sigma-Aldrich) counterstaining was performed for 10 minutes and sections were mounted

For Peer Review Only

using fluorescence mounting medium (ThermoFisher Scientific). Immunofluorescence analysis was performed using an Olympus DP71 fluorescence microscope fluorescence microscope.

Statistical Analysis

All statistical analyses were performed using GraphPad Prism 6.0 software. Mouse haematuria and albuminuria were analysed using two-way ANOVA, including time as a variable. All other comparisons between two groups were evaluated using the nonparametric Mann-Whitney U test. Differences were considered statistically significant when $p < 0.05$. Data shown represent mean values per experimental group ±SEM.

For Peer Review Only

REFERENCES

1. Mehrling T, Chen Y. The Alkylating-HDAC Inhibition Fusion Principle: Taking Chemotherapy to the Next Level with the First in Class Molecule EDO-S101. *Anti-Cancer Agents in Medicinal Chemistry.* 2016;16(1):20-28.
2. Little MA, Smyth L, Salama AD, et al. Experimental Autoimmune Vasculitis : An Animal Model of Anti-neutrophil Cytoplasmic Autoantibody-Associated Systemic Vasculitis. *The American Journal of Pathology.* 2009;174(4):1212-1220.
3. O'Reilly VP, Wong L, Kennedy C, et al. Urinary Soluble CD163 in Active Renal Vasculitis. *Journal of the American Society of Nephrology.* 2016.
4. Little MA, Bhangal G, Smyth CL, et al. Therapeutic Effect of Anti–TNF-α Antibodies in an Experimental Model of Anti-Neutrophil Cytoplasm Antibody–Associated Systemic Vasculitis. *Journal of the American Society of Nephrology.* 2006;17(1):160-169.
5. Xiao H, Heeringa P, Hu P, et al. Antineutrophil cytoplasmic autoantibodies specific for myeloperoxidase cause glomerulonephritis and vasculitis in mice. *The Journal of Clinical Investigation.* 2002;110(7):955-963.
6. Al-Ani B, Fitzpatrick M, Al-Nuaimi H, et al. Changes in urinary metabolomic profile during relapsing renal vasculitis. *Scientific Reports.* 2016;6:38074.

For Peer Review Only